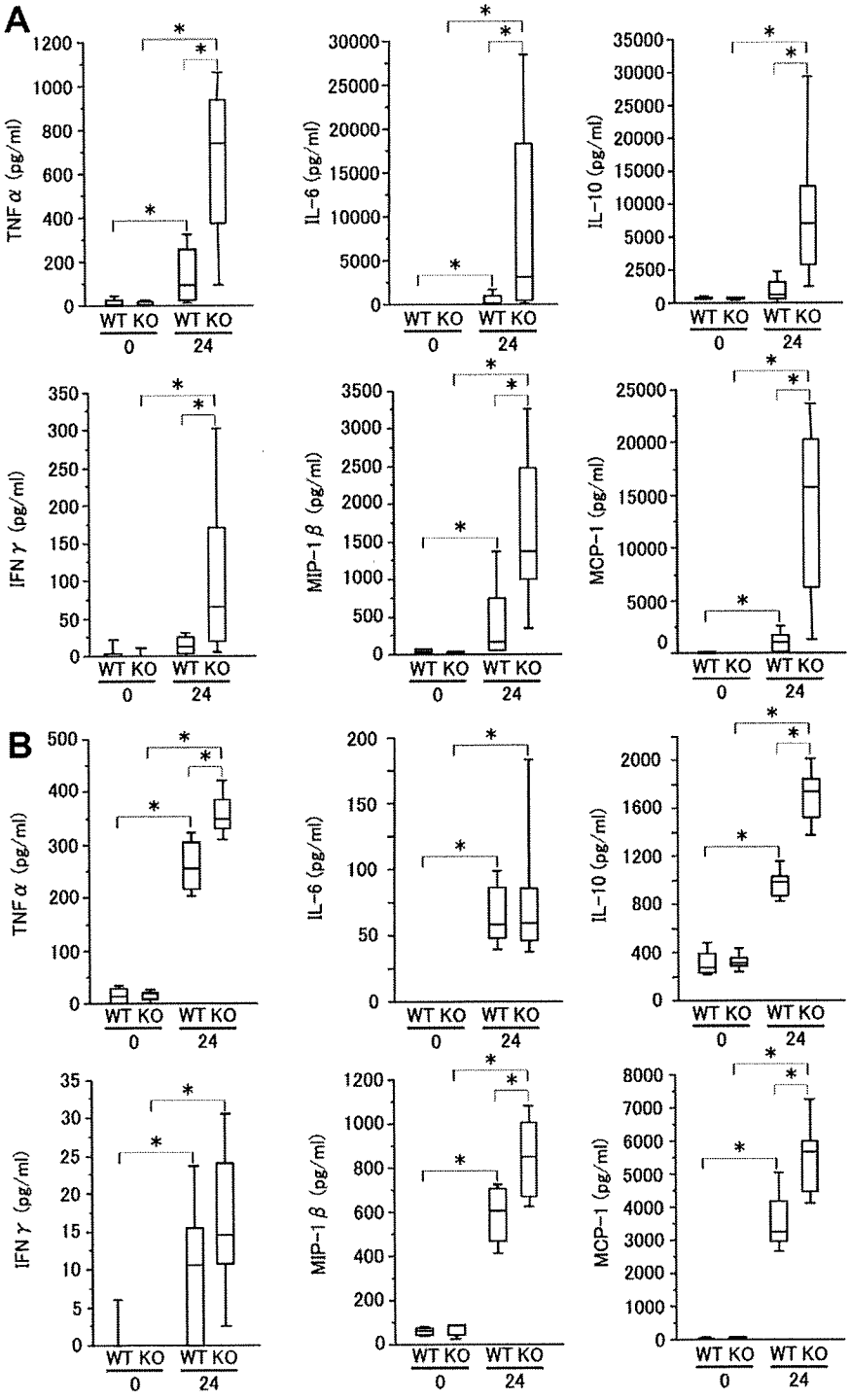

Fig. 4. Circulating cytokines before and after CLP or LPS injection. (A) L-STAT3 KO mice (KO) or wild-type littermates (WT) were treated with CLP (n = 8 in each group). Before and 24 hours after CLP, blood samples were obtained from mice and subjected to analysis of each cytokine indicated. *$P < 0.05$. (B) Mice were injected with 4 mg/kg of LPS (n = 8 in each group). Before and 24 hours after LPS injection, blood samples were obtained and subjected to the analysis of each cytokine indicated. *$P < 0.05$.

duced septic mice without affecting bacterial infection. L-STAT3 KO mice produced high levels of cytokines when injected with LPS, confirming that the absence of STAT3 signaling within hepatocytes induces a hyperinflammatory response even if the extent of the input stimuli remains constant. This phenomenon is similar to a previous report of macrophage-specific disruption of STAT3 in which serum cytokines such as TNF-α, IL-6, and IL-10 increased upon LPS stimulation.[22] In those mice, immune cells could not respond to IL-10, which potentially inhibit TNF-α production via STAT3 signaling, and thus produced high levels of TNF-α. Further study revealed those mice to be vulnerable to CLP-induced sepsis.[23,24] However, in our L-STAT3 KO mice, the levels of STAT3 in macrophage did not differ from control mice and produced the same amount of TNF-α in response to LPS (Fig. 1C-D). Thus, suppression of the inflammatory response in wild-type mice was critically

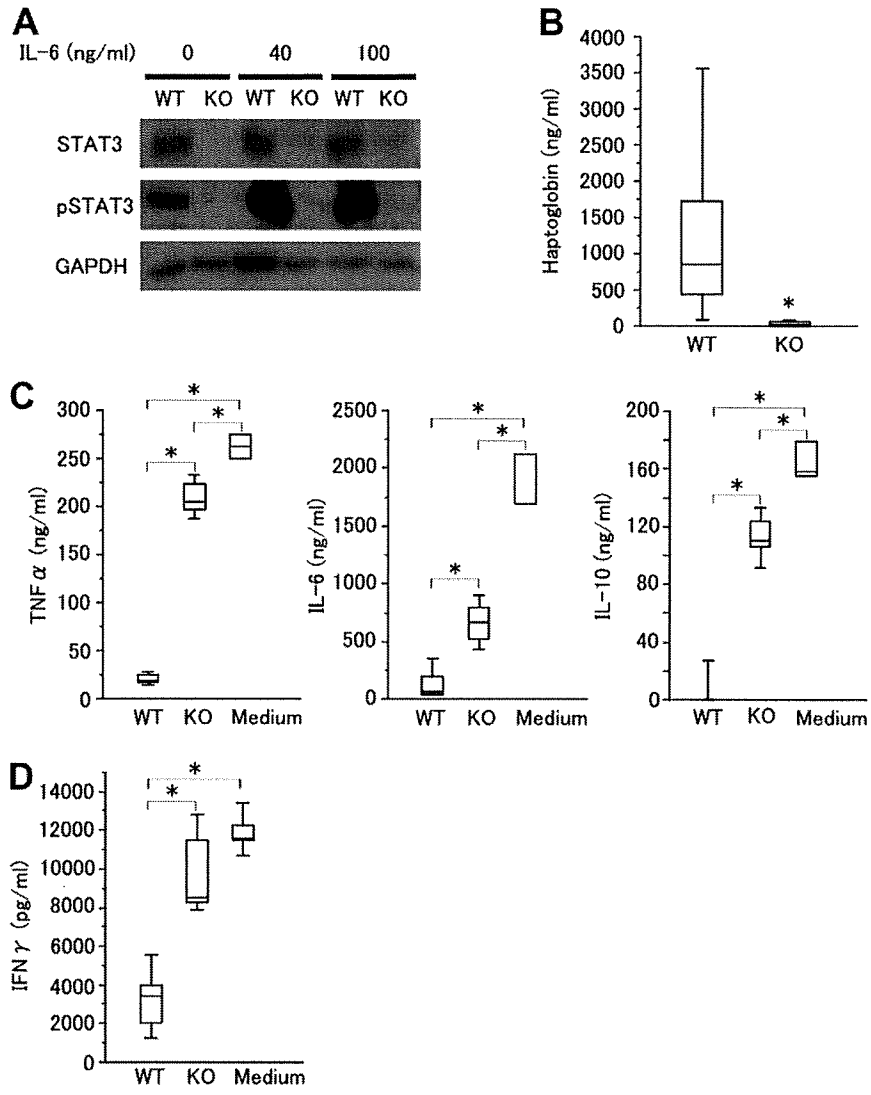

Fig. 5. Suppression of cytokine production from immune cells by hepatocyte culture supernatant. Hepatocytes were isolated from L-STAT3 KO (KO) or wild-type (WT) mice and cultured in the presence or absence of IL-6 for 2 hours (for western blot analysis) or 48 hours (for collection of culture supernatants). (A) STAT3 phosphorylation (pSTAT3) and STAT3 expression of hepatocytes via western blot analysis. GAPDH expression served as a control. Representative blots are shown. (B) Haptoglobin production from primary hepatocytes. Haptoglobin concentration was determined in the hepatocyte supernatants via ELISA. Comparison of haptoglobin production between knockout hepatocytes and wild-type hepatocytes ($n = 5$ mice/group) cultured in the absence of IL-6. $^*P < 0.05$. (C,D) Suppression of cytokine production in RAW cells or splenocytes by the hepatocyte supernatants. Hepatocytes were cultured for 48 hours. RAW cells (C) or splenocytes freshly isolated from wild-type mice (D) were cultured in the presence (KO or WT) or absence (Medium) of hepatocyte supernatants for 24 hours and then stimulated with LPS for another 24 hours. TNF-α, IL-6, IL-10, and IFN-γ production was determined via ELISA. $^*P < 0.05$.

dependent on hepatic STAT3 signaling. Indeed, in vitro analysis revealed that soluble factors from hepatocytes repress cytokine production from activated macrophage and splenocytes in a hepatic STAT3-dependent manner. Whereas research has established that STAT3 mediates a variety of effects on hepatocytes, including proliferation,[5] apoptosis protection,[6] and glucose metabolism,[7] the present study reveals that hepatic STAT3 has an important extrahepatic effect. This effect is activated by a variety of cytokines produced from immune cells such as IL-6 but, in turn, suppresses immune cell activation via production of soluble factors, providing a negative feedback loop. Thus, the present study describes a role of hepatic STAT3 in maintaining host homeostasis by negatively regulating the immune system.

APPs are liver plasma proteins whose levels of expression are either positively or negatively regulated by cytokines during inflammation. It has been established that STAT3 regulates the expression of most, if not all, APPs in the liver.[19] Consistent with this, L-STAT3 KO mice displayed impaired production of APPs in response to CLP (Fig. 2B). Some APPs such as C-reactive protein,[25] serum amyloid P,[26] and α2-macroglobulin[27] have been shown to bind bacteria and to positively or negatively affect their eradication. Several reports also suggest that APPs exert proinflammatory as well as anti-inflammatory effects.[25,28] C-reactive protein binds to the phosphocholine of some foreign pathogens as well as phospholipid constituents of damaged cells and can activate the complement system, whereas the antioxidants haptoglobin and hemopexin protect against reactive oxygen species. Thus, each APP has a unique role in the complex mechanism controlling infection-induced inflammation. The L-STAT3 KO mice used in the present study offer a unique model for identifying the net effect of STAT3-regulated APPs during the septic condition. Our work has revealed that the most prominent effect of STAT3-regulated APPs is suppression of the hyperinflammatory re-

sponse and lethality without an effect on bacterial infection. The soluble factors from hepatocytes that suppress cytokine production from immune cells are still unknown. Although there may be several substances involved in this phenomenon, one candidate might be haptoglobin, which was recently demonstrated to suppress TNF-α, IL-12, and IL-10 from human peripheral blood mononuclear cells in vitro.[29] We also obtained a similar finding that RAW cells produced a lesser amount of TNF-α upon LPS stimulation in the presence of haptoglobin (Supplementary Fig. 2). Identification of these substances may have important therapeutic implications for controlling the hyperinflammatory condition. Further study is needed to clarify this point.

The liver is one of the target organs of sepsis-induced multiple organ dysfunction syndrome. Evidence for this comes from the fact that CLP mice or LPS mice showed liver injury as evidenced by increases in serum ALT and TUNEL-positive hepatocytes scattered in the liver lobule. Furthermore, L-STAT3 KO mice displayed more hepatocyte apoptosis in mice subjected to CLP or LPS injection. Previous research has indicated that the absence of hepatic STAT3 renders hepatocytes more vulnerable to Fas-mediated apoptosis.[6] It is possible that STAT3-null hepatocytes are more vulnerable to apoptosis in the septic model. However, at the same time, L-STAT3 KO mice showed higher levels of proinflammatory cytokines such as TNF-α, which is a direct inducer of hepatocyte apoptosis. In our model, it is difficult to differentiate which contributed more to increased liver injury: the decrease in apoptosis resistance or the increase in proinflammatory cytokine. It can be said that the increase of proinflammatory cytokines is presumably one of the causes, but not a result, of liver injury. In addition, as discussed in the Results section, liver injury was relatively modest and probably not a direct cause of animal death.

In the present study, the lack of hepatic STAT3 caused increased mortality in CLP mice. Although we did not address the direct link between hypercytokinemia and animal death, accumulating evidence suggests that an increase in a variety of cytokines is involved in lethality in CLP mice. For example, it was shown that IL-6 plays an important role in the increased expression of the C5a receptor in the lung, liver, kidney, and heart during the development of sepsis in CLP mice and that interception of IL-6 leads to reduced expression of the C5a receptor and improved survival.[30] In addition, enforced expression of the IL-6 gene in wild-type mice led to high mortality (unpublished data). TNF-α and other cytokines increase expression of inducible nitric oxide synthase, and increased production of nitric oxide causes further vascular instability and may also contribute to the direct myocardial depression that occurs in sepsis.[31] Thus, dysregulation of cytokines may be harmful for host organs and is probably linked to animal death.

The present study revealed an important role of hepatocytes in repressing the hyperinflammatory response in pathologic conditions. This raises the possibility that hyperinflammation may be ill-controlled when liver function is severely impaired. Although sepsis itself is not a frequent cause of liver failure, it is a serious complication of acute or chronic liver failure. Systemic inflammatory response syndrome is an important determinant of prognosis in fulminant hepatitis.[12] Sepsis originating from spontaneous bacterial peritonitis or renal infection is one of the causes of patient death with decompensated cirrhosis.[13] In patients with limited function of the liver, possible impairment of STAT3-regulated hepatocyte function may be involved in their poor prognosis when complicated with severe inflammation. Careful liver-supporting therapy or early liver transplantation should be considered not only for maintaining liver function but also from the aspect of controlling dysregulated hyperinflammatory responses.

In conclusion, hepatic STAT3 represses systemic hyperinflammatory response by stimulating hepatic production of soluble substances that can attenuate immune cell overactivation and also improves host survival during septic condition. This sheds light on hepatocytic STAT3 as a negative regulator for immune cell overactivation and its role in host defense during systemic severe inflammation.

References

1. Akira S. IL-6-regulated transcription factors. Int J Biochem Cell Biol 1997; 29:1401-1418.
2. Akira S, Nishio Y, Inoue M, Wang XJ, Wei S, Matsusaka T, et al. Molecular cloning of APRF, a novel IFN-stimulated gene factor 3 p91-related transcription factor involved in the gp130-mediated signaling pathway. Cell 1994;77:63-71.
3. Zhong Z, Wen Z, Darnell JE Jr. Stat3: a STAT family member activated by tyrosine phosphorylation in response to epidermal growth factor and interleukin-6. Science 1994;264:95-98.
4. Takeda K, Noguchi K, Shi W, Tanaka T, Matsumoto M, Yoshida N, et al. Targeted disruption of the mouse Stat3 gene leads to early embryonic lethality. Proc Natl Acad Sci U S A 1997;94:3801-3804.
5. Li W, Liang X, Kellendonk C, Poli V, Taub R. STAT3 contributes to the mitogenic response of hepatocytes during liver regeneration. J Biol Chem 2002;277:28411-28417.
6. Haga S, Terui K, Zhang HQ, Enosawa S, Ogawa W, Inoue H, et al. Stat3 protects against Fas-induced liver injury by redox-dependent and -independent mechanisms. J Clin Invest 2003;112:989-998.
7. Inoue H, Ogawa W, Ozaki M, Haga S, Matsumoto M, Furukawa K, et al. Role of STAT-3 in regulation of hepatic gluconeogenic gene and carbohydrate metabolism in vivo. Nat Med 2004;10:168-174.
8. Angus DC, Linde-Zwirble WT, Lidicker J, Clermont G, Carcillo J, Pinsky MR. Epidemiology of severe sepsis in the United States: analysis of incidence, outcome, and associated costs of care. Crit Care Med 2001;29: 1303-1310.
9. Cohen J. The immunopathogenesis of sepsis. Nature 2002;420:885-891.

10. Hotchkiss RS, Karl IE. The pathophysiology and treatment of sepsis. N Engl J Med 2003;348:138-150.
11. Wang P, Chaudry IH. Mechanism of hepatocellular dysfunction during hyperdynamic sepsis. Am J Physiol 1996;270:R927-R938.
12. Rolando N, Wade J, Davalos M, Wendon J, Philpott-Howard J, Williams R. The systemic inflammatory response syndrome in acute liver failure. HEPATOLOGY 2000;32:734-739.
13. Fasolato S, Angeli P, Dallagnese L, Maresio G, Zola E, Mazza E, et al. Renal failure and bacterial infections in patients with cirrhosis: epidemiology and clinical features. HEPATOLOGY 2007;45:223-229.
14. Takeda K, Kaisho T, Yoshida N, Takeda J, Kishimoto T, Akira S. Stat3 activation is responsible for IL-6-induced T cell proliferation through preventing apoptosis: generation and characterization of T cell-specific Stat3-deficient mice. J Immunol 1998;161:4652-4660.
15. Takehara T, Tatsumi T, Suzuki T, Rucker EB 3rd, Hennighausen L, Jinushi M, et al. Hepatocyte-specific disruption of Bcl-xL leads to continuous hepatocyte apoptosis and liver fibrotic responses. Gastroenterology 2004;127:1189-1197.
16. Fink MP, Heard SO. Laboratory models of sepsis and septic shock. J Surg Res 1990;49:186-196.
17. Takehara T, Uemura A, Tatsumi T, Suzuki T, Kimura R, Shiotani A, et al. Natural killer cell-mediated ablation of metastatic liver tumors by hydrodynamic injection of IFNα gene to mice. Int J Cancer 2007;120:1252-1260.
18. Andrejko KM, Chen J, Deutschman CS. Intrahepatic STAT-3 activation and acute phase gene expression predict outcome after CLP sepsis in the rat. Am J Physiol 1998;275:G1423-G1429.
19. Alonzi T, Maritano D, Gorgoni B, Rizzuto G, Libert C, Poli V. Essential role of STAT3 in the control of the acute-phase response as revealed by inducible gene inactivation in the liver. Mol Cell Biol 2001;21:1621-1632.
20. Zhang Z, Fuentes NL, Fuller GM. Characterization of the IL-6 responsive elements in the gamma fibrinogen gene promoter. J Biol Chem 1995;270:24287-24291.
21. Kim H, Baumann H. The carboxyl-terminal region of STAT3 controls gene induction by the mouse haptoglobin promoter. J Biol Chem 1997;272:14571-14579.
22. Takeda K, Clausen BE, Kaisho T, Tsujimura T, Terada N, Forster I, et al. Enhanced Th1 activity and development of chronic enterocolitis in mice devoid of Stat3 in macrophages and neutrophils. Immunity 1999;10:39-49.
23. Matsukawa A, Takeda K, Kudo S, Maeda T, Kagayama M, Akira S. Aberrant inflammation and lethality to septic peritonitis in mice lacking STAT3 in macrophages and neutrophils. J Immunol 2003;171:6198-6205.
24. Matsukawa A, Kudo S, Maeda T, Numata K, Watanabe H, Takeda K, et al. Stat3 in resident macrophages as a repressor protein of inflammatory response. J Immunol 2005;175:3354-3359.
25. Gabay C, Kushner I. Acute-phase proteins and other systemic responses to inflammation. N Engl J Med 1999;340:448-454.
26. Noursadeghi M, Bickerstaff MC, Gallimore JR, Herbert J, Cohen J, Pepys MB. Role of serum amyloid P component in bacterial infection: protection of the host or protection of the pathogen. Proc Natl Acad Sci U S A 2000;97:14584-14589.
27. Hochepied T, Van Leuven F, Libert C. Mice lacking alpha2-macroglobulin show an increased host defense against Gram-negative bacterial sepsis, but are more susceptible to endotoxic shock. Eur Cytokine Netw 2002;13:86-91.
28. Tilg H, Dinarello CA, Mier JW. IL-6 and APPs: anti-inflammatory and immunosuppressive mediators. Immunol Today 1997;18:428-432.
29. Arredouani MS, Kasran A, Vanoirbeek JA, Berger FG, Baumann H, Ceuppens JL. Haptoglobin dampens endotoxin-induced inflammatory effects both in vitro and in vivo. Immunology 2005;114:263-271.
30. Riedemann NC, Neff TA, Guo RF, Bernacki KD, Laudes IJ, Sarma JV, et al. Protective effects of IL-6 blockade in sepsis are linked to reduced C5a receptor expression. J Immunol 2003;170:503-507.
31. Landry DW, Oliver JA. The pathogenesis of vasodilatory shock. N Engl J Med 2001;345:588-595.

Natural killer cell and hepatic cell interaction via NKG2A leads to dendritic cell-mediated induction of CD4$^+$ CD25$^+$ T cells with PD-1-dependent regulatory activities

Masahisa Jinushi, Tetsuo Takehara, Tomohide Tatsumi, Shinjiro Yamaguchi, Ryotaro Sakamori, Naoki Hiramatsu, Tatsuya Kanto, Kazuyoshi Ohkawa and Norio Hayashi

Department of Gastroenterology and Hepatology, Osaka University Graduate School of Medicine, Osaka, Japan

doi:10.1111/j.1365-2567.2006.02479.x
Received 24 June 2006; revised 24 August 2006; accepted 24 August 2006.
Correspondence: Norio Hayashi MD, Department of Gastroenterology and Hepatology, Osaka University Graduate School of Medicine, 2–2 Yamada-oka, Suita, Osaka 565-0871, Japan.
Email: hayashin@gh.med.osaka-u.ac.jp
Senior author: Tetsuo Takehara, email: takehara@gh.med.osaka-u.ac.jp

Summary

Natural killer (NK) cells have the ability to control dendritic cell (DC)-mediated T cell responses. However, the precise mechanisms by which NK receptor-mediated regulation of NK cells determines the magnitude and direction of DC-mediated T cell responses remain unclear. In the present study, we applied an *in vitro* co-culture system to examine the impact of NK cells cultured with hepatic cells on DC induction of regulatory T cells. We found that interaction of NK cells and non-transformed hepatocytes (which express HLA-E) via the NKG2A inhibitory receptor resulted in priming of DCs to induce CD4$^+$ CD25$^+$ T cells with regulatory properties. NKG2A triggering led to characteristic changes of the cytokine milieu of co-cultured cells; an increase in the transforming growth factor (TGF)-β involved in the generation of this specific type of DC, and a decrease in the tumour necrosis factor-α capable of antagonizing the effect of TGF-β. The regulatory cells induced by NK cell-primed DCs exert their suppressive actions through a negative costimulator programmed death-1 (PD-1) mediated pathway, which differs from freshly isolated CD4$^+$ CD25$^+$ T cells. These findings provide new insight into the role of NK receptor signals in the DC-mediated induction of regulatory T cells.

Keywords: NK receptor; regulatory T cell; HLA-E; liver; HCV

Introduction

CD4$^+$ CD25$^+$ regulatory T (Treg) cells have been identified as the main suppressors of immune responses.[1–5] Although the mechanisms by which CD4$^+$ CD25$^+$ Treg cells exert their suppressive actions have not been fully elucidated, negative costimulatory signals via cytotoxic T lymphocyte antigen-4 (CTLA-4) or inducible costimulator (ICOS)-mediated signals, have been suggested to play a key role in the activation of CD4$^+$ CD25$^+$ Treg cells.[6,7] Programmed death-1 (PD-1), another molecule identified as a negative costimulatory receptor, has also serves as a negative regulator for effector immune responses.[8] Recent reports have demonstrated that PD-1 is expressed in CD4$^+$ CD25$^+$ Treg cells, suggesting its potential roles in the regulation of T cell tolerance.[9] However, the precise roles of PD-1 in CD4$^+$ CD25$^+$ Treg cell functions remain elusive.

The mechanisms by which CD4$^+$ CD25$^+$ Treg cells are generated have been extensively investigated. Dendritic cells (DCs), the sentinels between innate and adaptive immunity, have recently emerged as candidate cells involved in the differentiation and/or activation of CD4$^+$ CD25$^+$ Treg cells.[10] Various kinds of factors have been identified as involved in DC induction of CD4$^+$ CD25$^+$ Treg cells. Mouse immature DC promotes the differentiation of CD4$^+$ CD25$^+$ Treg cells through the DEC 205-mediated targeting of self-antigen in the steady state.[10,11] The immune regulatory cytokines interleukin (IL)-10/transforming growth factor (TGF)-β have also been reported to play important roles in DC generation and activation of CD4$^+$ CD25$^+$ Treg cells.[12–14]

Abbreviations: CTLA-4, cytotoxic T lymphocyte antigen-4; DC, dendritic cell; ELISA, enzyme-linked immunosorbent assay; GITR, glucocorticoid-induced TNF receptor; HCV, hepatitis C virus; HLA, human leucocyte antigen; NH, human non-transformed hepatocyte; NK, natural killer; PD-1, programmed death-1; PDL-1, programmed death ligand 1; PBMC, peripheral blood mononuclear cell; Treg, regulatory T.

Several lines of evidence have revealed that natural killer (NK) cell-mediated innate immunity regulates DC functions to determine the direction and magnitude of adaptive T cell immunity.[15–18] It has also been established that NK cell function is regulated by positive and negative signals through their receptor and ligand interactions.[19] We previously reported that, upon exposure to non-transformed hepatocytes (NHs), IL-2-primed NK cells negatively regulated DC functions, which appeared to be dependent on NKG2A inhibitory signals during co-culture of NK cells and NHs. Immunosuppressive cytokines such as IL-10 and TGF-β, but not direct NK–DC contact, were responsible for this action.[20] However, it remains unclear whether these NK/hepatocyte co-cultures can also influence the induction as well as activation of $CD4^+$ $CD25^+$ Treg cells.

In the present study, we investigated whether DCs stimulated with the co-culture supernatant of IL-2-prestimulated NK cells and NHs can modulate Treg cell functions. We found that TGF-β produced from NK cell/hepatocyte co-culture via NKG2A activation is responsible for modulating DCs to induce and maintain regulatory phenotypes and functions of $CD4^+$ $CD25^+$ Treg cells. Furthermore, the generated $CD4^+$ $CD25^+$ Treg cells suppressed T cell activation via interaction between PD-1 and programmed death ligand 1 (PDL-1). These findings represent new evidence that NK receptor-mediated modulation of NK cells may dictate DC-induced adaptive immunity toward an immunogenic or tolerogenic status via induction of Treg cells.

Materials and methods

Antibodies

Anti-NKG2A monoclonal antibody (mAb) (Z199), PC5-labelled CD25 mAb or isotype-matched control IgG1 and IgG2a mAb were purchased from Beckmann-Coulter (Fullerton, CA). Anti-IL-10, anti-TGF-β, anti-CTLA-4, anti-GITR (glucocorticoid-induced TNF receptor) and anti-PD-1 polyclonal Abs were purchased from R & D Systems (Minneapolis, MN) and phycoerythrin (PE)-labelled mAb CTLA-4 from BD Biosciences (San Jose, CA). Anti-HLA-E mAb 3D12 was kindly provided by Dr E. Geraghty (Fred Hutchinson Cancer Research Institute, Seattle, WA) and used as reported previously.[21] Anti-MIC mAb 6D4, anti-ULBP1 mAb 3F1 and anti-ULBP2 mAb DH1 were kindly provided by Drs T. Spies and V. Groh (Fred Hutchinson Cancer Research Institute) and used as reported previously.[22]

Human hepatic cells

Human non-transformed hepatocytes (NHs) derived from mixed heterogeneous donors were purchased from the Applied Cell Biology Research Institute (Kirkland, WA) and cultured in CS-C complete medium according to the manufacturer's instructions.

Isolation of peripheral blood lymphocyte populations

Resting NK cells ($CD56^+$ $CD3^+$), naive $CD4^+$ T cells ($CD45RA^+$ RO^+) or $CD8^+$ T cells were isolated from peripheral blood mononuclear cells (PBMCs) with a positive cell isolation kit according to the manufacturer's protocol (Miltenyi Biotec, Bergisch Gladbach, Germany). $CD4^+$ $CD25^+$ T cells were further separated from naive $CD4^+$ T cells using anti-CD25 microbeads (Miltenyi Biotech). Their purity was >90% by flow cytometry. Informed consent was obtained from all blood donors.

Generation of monocyte-derived DC

Monocytes were isolated by plastic adherence from PBMCs and cultured in RPMI-1640 supplemented with granulocyte–macrophage colony stimulating factor (GM-CSF) (PeproTech, London, UK) and IL-4 (PeproTech). At day 6, they were stimulated with or without the co-culture supernatant of NK cells and hepatic cells. At day 7, non-adherent cells were harvested and used as described below.

Stimulation of DCs by co-culture supernatants of NK cells and hepatic cells

Freshly isolated NK cells were cultured with or without IL-2 for 24 hr. IL-2-prestimulated or non-stimulated NK cells were seeded in 24-well plates and then co-cultured for 24 hr with NHs (1×10^5 cells/well), respectively. Monocyte-derived DCs were cultured for 24 hr with 1 ml of the co-culture supernatant of IL-2-prestimulated NK cells and NHs (NH/IL-2 NK-primed DC). In some experiments, anti-NKG2A mAb (Z199) or isotype-matched control Ab was added during the co-cultures of NK cells and hepatic cells. Z199 mAb was previously confirmed to block the NKG2A-mediated signal.[23] In some experiments, the supernatant of NK/hepatic cell co-cultures was also treated with anti-IL-10 or anti-TGF-β neutralizing Ab and used for DC stimulation for 24 hr. In some experiments, tumour necrosis factor (TNF)-α, TGF-β or both were used for DC stimulation for 24 hr.

Isolation of $CD4^+$ $CD25^+$ T cells

DCs (1×10^5) were stimulated for 24 hr with the supernatant obtained from the co-cultured medium. After washing three times, DCs were cultured with allogeneic $CD4^+$ T cells for 48 hr; $CD4^+$ $CD25^+$ fractions were isolated from DC and $CD4^+$ co-culture and subjected to further analysis. $CD4^+$ $CD25^+$ fractions were also isolated

from PBMCs and cultured with 1 μg/ml plate-bound anti-CD3 mAb (UCHT1; Beckmann-Coulter) for 24 hr to efficiently induce their suppressive properties as described previously.[3] These cells are referred to as natural $CD4^+$ $CD25^+$ T cells.

Flow cytometry

The expression of NK inhibitory ligands (human leucocyte antigen, HLA, class I, HLA-E) was examined on NHs by using w6/32 or 3D12, respectively. MIC, ULBP1 or ULBP2 expression on hepatocytes was also evaluated by mAb 6D4, 3F1 or DH1, respectively. For $CD4^+$ $CD25^+$ T cell staining, the cells were costained with PC5-labelled CD25 mAb with PE-labelled mAb of CTLA-4, GITR or PD-1 polyclonal Ab. The cells were analysed by flow cytometry using a fluorescence-activated cell sorter (FACScan) system, and data analysis was performed using CELLQUEST software.

Measurements of cytokine production in culture supernatant

The culture supernatants of interferon (IFN)-γ, TNF-α, IL-10 and TGF-β were examined using enzyme-linked immunosorbent assay (ELISA) kits according to the manufacturers' instructions (IFN-γ, TNF-α and IL-10, Endogen, Tokyo, Japan; TGF-β, R & D Systems).

Analysis of Foxp3 mRNA expression

Polymerase chain reaction (PCR) analysis was performed to determine Foxp3 mRNA expression of $CD4^+$ T cells using a commercial PCR panel according to the manufacturer's instructions (Gibco BRL, Rockville, MD). The following primers were used: 5′-CCCACTTACAGGCACT CCTC-3′ (forward) and 5′-CTTCTCCTTCTCCAGCAC CA-3′ (reverse).[24] Amplification was carried out for 35 cycles of 20 seconds at 95°, 20 seconds at 58 ° and 30 seconds at 72°. As a control for the integrity of mRNA, primers specific for GAPDH (glyceraldehyde 3-phosphate dehydrogenase) were used as follows: 5′-GCCACCCAGAAGACTGTGGATGGC-3′ (forward) and 5′-CATGTAGGCCATGAGGTCCACCAC-3′ (reverse). The PCR products were analysed by ethidium bromide-stained 1·5% agarose gel electrophoresis.

Analysis of $CD4^+$ $CD25^+$ T cell suppressor functions

DCs (5×10^4/well) were cultured with allogeneic $CD4^+$ T cells (5×10^5/well) for 48 hr, after which $CD4^+$ $CD25^+$ T cells were isolated from the co-cultured cells. $CD4^+$ $CD25^-$ T cells were freshly isolated from the same donors and activated with 1 μg/ml plate-bound anti-CD3 mAb in the presence or absence of autologous $CD4^+$ $CD25^+$ T cells for 48 hr. The ability of $CD4^+$ $CD25^+$ T cells to suppress proliferation and IFN-γ production of activated $CD4^+$ $CD25^-$ T cells was determined by [^{3}H]thymidine incorporation and ELISA assay, respectively. To further examine the mechanisms of $CD4^+$ $CD25^+$ T cell suppressive actions, neutralizing Ab of IL-10 or TGF-β, anti-CTLA-4, anti-GITR or anti-PD-1 was added at the beginning of $CD4^+$ $CD25^+$ T cell and $CD4^+$ $CD25^-$ T cell co-cultures.

Statistical analysis

Comparisons between groups were analysed by *t*-test with Welch's correction or ANOVA for experiments with more than two subgroups. Differences were considered significant when the *P*-value was $< 0{\cdot}05$.

Results

IL-2-primed NK cells upon exposure to NH-modulated DCs on the induction of regulatory $CD4^+$ $CD25^+$ T cells

Natural $CD4^+$ $CD25^+$ T cells from human peripheral blood lymphocytes (PBLs) expressed CTLA-4 and GITR, both of which have been identified as regulatory markers,[6,25] but did not express PD-1 (Fig. 1a). To examine whether DCs can modulate the expression of these regulatory markers on $CD4^+$ $CD25^+$ T cells, we stimulated monocyte-derived DCs for 24 hr, either by the culture supernatant of IL-2-stimulated NK cells (IL-2 NK) or by the co-culture supernatant of NH/IL-2 NK. After washing, the resulting DCs were cultured for 48 hr with $CD4^+$ T cells isolated from allogeneic donors. $CD4^+$ $CD25^+$ T cells were isolated from the DC and $CD4^+$ T cell co-culture and subjected to analysis for regulatory markers. The expression levels of CTLA-4 and GITR decreased on $CD4^+$ $CD25^+$ T cells after stimulation of IL-2 NK-primed DCs (Fig. 1b). By contrast, $CD4^+$ $CD25^+$ T cells stimulated with NH/IL-2 NK-primed DCs remained positive for CTLA-4 and GITR on their surface. Of note is the finding that PD-1 was induced on these cells, showing their phenotypic properties to differ from natural $CD4^+$ $CD25^+$ T cells (Fig. 1b, c). The induction of PD-1 on $CD4^+$ $CD25^+$ T cells was further confirmed when IL-2NK/NH-primed DCs from different donors were used as stimulators (Fig. 1d). The supernatant of NH without NK cells had little effect on phenotypic changes of $CD4^+$ $CD25^+$ T cells by DCs (data not shown).

The forkhead transcription factor Foxp3 has been recently identified as a master gene for defining Treg cells.[26] We therefore performed reverse transcription-PCR (RT-PCR) analysis of $CD4^+$ T cells to evaluate the mRNA expression of Foxp3. Foxp3 expression was detected in natural $CD4^+$ $CD25^+$ T cells. When $CD4^+$ T cells were

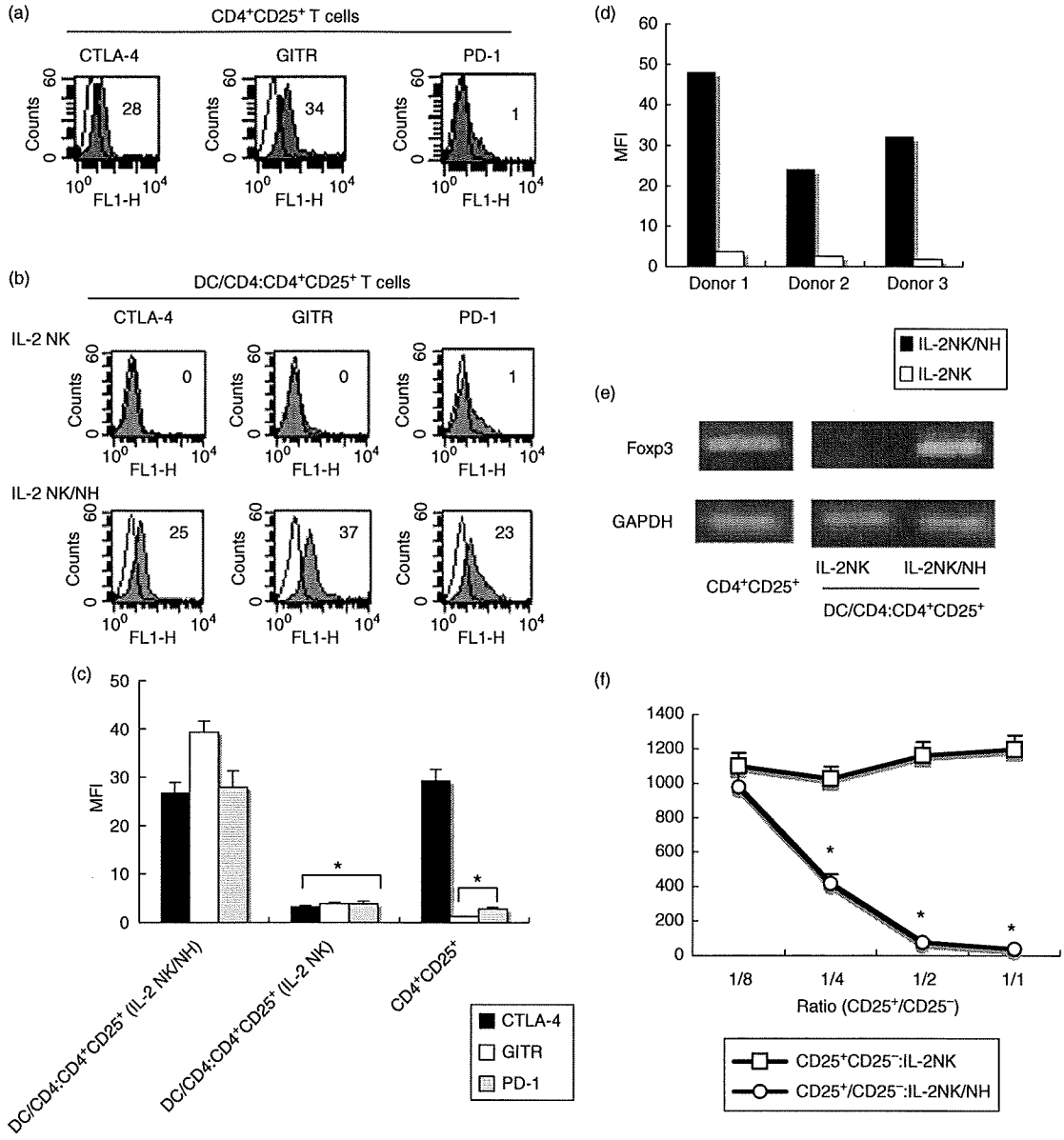

Figure 1. Human non-transformed hepatocyte (NH) modulation of activated natural killer (NK) cells endows dendritic cells (DCs) with the ability to induce $CD4^+$ $CD25^+$ regulatory T cells. (a) Freshly isolated $CD4^+$ $CD25^+$ T cells were cultured in the presence of plate-bound anti-CD3 antibody (Ab) for 24 hr, and then subjected to flow cytometry to examine their expression of cytotoxic T lymphocyte antigen-4 (CTLA-4), glucocorticoid-induced TNF receptor (GITR) and programmed death-1 (PD-1) (closed histograms). Open histograms represent the staining of control Ab. Numbers on the upper right indicate the mean fluorescence intensity (MFI) of each type of stained cells. (b) NK cells were preactivated with 50 ng/ml interleukin (IL)-2, and co-cultured in the absence (IL-2 NK) or presence (IL-2 NK/NH) of NHs at a ratio of 1 : 1 for 24 hr. DCs (1×10^5) were stimulated for 24 hr with the supernatant obtained from the co-cultured medium. After washing three times, DCs were cultured with allogeneic $CD4^+$ T cells for 48 hr. $CD4^+$ $CD25^+$ fractions were isolated from the DC/$CD4^+$ T co-culture and subjected to flow cytometry for expression of CTLA-4, GITR or PD-1 (closed histograms). Open histograms show isotype control staining. Numbers on the upper right indicate the MFI of each type of stained cell. (c) All experiments in (a) and (b) were performed three times and the composite results with statistical analysis are shown as the MFI of the staining cells. $^*P < 0{\cdot}05$ vs. responses of IL-2 NK/NH group. The experiment was performed with a different set of donors and similar results were obtained. (d) PD-1 expression on $CD4^+$ $CD25^+$ T cells stimulated with allogeneic DCs from three different donors, shown as the MFI. (e) $CD4^+$ $CD25^+$ T cells were prepared as described above. The mRNA expression of Foxp3 and GAPDH (glyceraldehyde 3-phosphate dehydrogenase) was examined by reverse transcription-polymerase chain reaction (RT-PCR). (f) $CD4^+$ $CD25^+$ fractions were isolated from DC/$CD4^+$ T cell co-cultures. Different numbers of these $CD4^+$ $CD25^+$ T cells were co-cultured with freshly isolated autologous $CD4^+$ $CD25^-$ T cells (1×10^5/well) in the presence of plate-bound anti-CD3 Ab ($CD4^+$ $CD25^+$/$CD4^+$ $CD25^-$). The anti-CD3 Ab-activated $CD4^+$ $CD25^-$ T cells alone were used as a positive control ($CD4^+$ $CD25^-$). IFN-γ was measured for each supernatant obtained after 48 hr of co-culture by enzyme-linked immunosorbent assay. $^*P < 0{\cdot}05$.

stimulated with IL-2 NK-primed DCs for 24 hr, Foxp3 was not expressed on $CD4^+$ $CD25^+$ T cells. By contrast, they dominantly transcribed Foxp3 at levels comparable with those of natural $CD4^+$ $CD25^+$ T cells when stimulated with NH/IL-2 NK-primed DCs (Fig. 1e). Taken together, $CD4^+$ $CD25^+$ T cells, when stimulated by NH/IL-2 NK-primed DCs, maintained regulatory phenotypes such as CTLA-4, GITR and Foxp3, and properties distinct from those of natural $CD4^+$ $CD25^+$ Treg cells in terms of PD-1 expression.

$CD4^+$ $CD25^+$ T cells on stimulation of NH/IL-2 NK-primed DC suppressed effector cell functions

We next analysed the functions of $CD4^+$ $CD25^+$ T cells stimulated by NH/IL-2 NK-primed DC. $CD4^+$ $CD25^+$ T cells were co-cultured for 72 hr with $CD4^+$ $CD25^-$ T cells freshly isolated from the same donors. During the co-cultures, $CD4^+$ $CD25^-$ T cells were stimulated with plate-bound anti-CD3 Ab. The $CD4^+$ $CD25^+$ T cells induced by NH/IL-2 NK-primed DCs dose-dependently suppressed the proliferation of co-cultured cells, whereas those induced by IL-2 NK-primed DC did not (data not shown). $CD4^+$ $CD25^+$ T cells induced by NH/IL-2 NK-primed DCs also dose-dependently inhibited IFN-γ production of the co-cultured cells, by contrast with those induced by IL-2 NK-primed DCs (Fig. 1f). The suppressive activities of these $CD4^+$ $CD25^+$ Treg cells were similar to those of natural $CD4^+$ $CD25^+$ Treg cells (data not shown). These results demonstrate that $CD4^+$ $CD25^+$ T cells induced by NH/IL-2 NK-primed DCs exert suppressive actions to effector cell functions, consistent with their expression of regulatory markers. Taken together, these results indicated that NK cell modulation of DCs leads to the $CD4^+$ $CD25^+$ Treg cell-mediated suppression of effector cell responses when NK cells encounter hepatocytes.

NKG2A signal of NK cells is responsible for the modulation of DCs to activate $CD4^+$ $CD25^+$ Treg cells

We examined the expression of various ligands for NK cell receptors on NHs. NHs expressed HLA-E, the ligand of NKG2A, but did not express NKG2D receptor ligands, MIC and ULBP1-2 (Fig. 2a). Given our previous findings that NHs negatively regulated IL-2 NK-mediated modulation of DC functions through the interaction of the NKG2A inhibitory receptor and its ligand HLA-E,[20] we evaluated the role of these receptor signals in the induction of $CD4^+$ $CD25^+$ Treg cells by DCs. When anti-NKG2A Ab was added during the co-culture of NH and IL-2 NK and DCs were stimulated with the resultant supernatant, the expression of CTLA-4, GITR and PD-1 was diminished on $CD4^+$ $CD25^+$ T cells (Fig. 2b, c). NKG2A blockade also suppressed PD-1 expression on $CD4^+$ $CD25^+$ T cells stimulated with IL-2NK/NH-primed DCs from three different donors (Fig. 2d). The anti-NKG2A neutralizing Ab treatment also abrogated Foxp3 expression in $CD4^+$ $CD25^+$ Treg cells (Fig. 2e). Moreover, the blockade of NKG2A signals during NH and IL-2 NK co-cultures resulted in inhibition of the DC ability to induce $CD4^+$ $CD25^+$ T cells with regulatory functions; these $CD4^+$ $CD25^+$ T cells did not suppress proliferation or IFN-γ production (Fig. 2f and data not shown) of $CD4^+$ $CD25^-$ T cells. Altogether, the activation of NKG2A inhibitory signals during NK cell and hepatocyte interaction was required for the DC induction of $CD4^+$ $CD25^+$ T cells with regulatory phenotypes and functions.

Change of cytokine milieu, triggered by NKG2A signals, plays a critical role in DC-mediated induction of $CD4^+$ $CD25^+$ Treg cells

TNF-α has been well known as a critical factor for NK cell-mediated maturation of DCs.[27] By contrast, IL-10 and TGF-β are known to act as suppressive factors of effector immune responses, and their roles in modulating DCs for Treg cell induction has recently been validated.[12–14] These findings led us to evaluate the change in cytokine production patterns in NH and IL-2 NK co-cultures in the presence or absence of anti-NKG2A Ab. ELISA data showed that the production of IFN-γ and TNF-α from NH and IL-2 NK co-cultures were substantially increased in the presence of anti-NKG2A Ab. By contrast, the addition of NKG2A masking Ab during the co-culture resulted in the marked reduction of IL-10 and TGF-β from co-cultured cells (Fig. 3a).

We next examined whether these changes of cytokine profiles were responsible for the DC induction of the $CD4^+$ $CD25^+$ Treg cells. For this purpose, the NH and IL-2 NK co-culture supernatant was treated with neutralizing Ab of IL-10 or TGF-β before DC stimulation, and suppressive activity was evaluated by analysing $CD4^+$ $CD25^+$ T cells obtained from $CD4^+$ and DC mixtures. The neutralization of IL-10 did not reverse the suppressive actions of $CD4^+$ $CD25^+$ Treg cells, but the blockade of TGF-β led to reversal of $CD4^+$ $CD25^+$ Treg cell activities (Fig. 3b).

We directly examined the effect of TGF-β on the modulation of DC ability to induce $CD4^+$ $CD25^+$ Treg cells. TGF-β endowed DCs with the ability to induce $CD4^+$ $CD25^+$ Treg cells. TNF-α inhibited TGF-β-mediated DC induction of $CD4^+$ $CD25^+$ Treg cells (Fig. 3c). By contrast, IFN-γ had little effect on the modulation of DC by TGF-β (data not shown). Taken together, these results strongly suggest that increased TGF-β and decreased TNF-α production, the change of cytokine profiles mediated by the NKG2A signals, are involved in DC-mediated $CD4^+$ $CD25^+$ Treg cell induction.

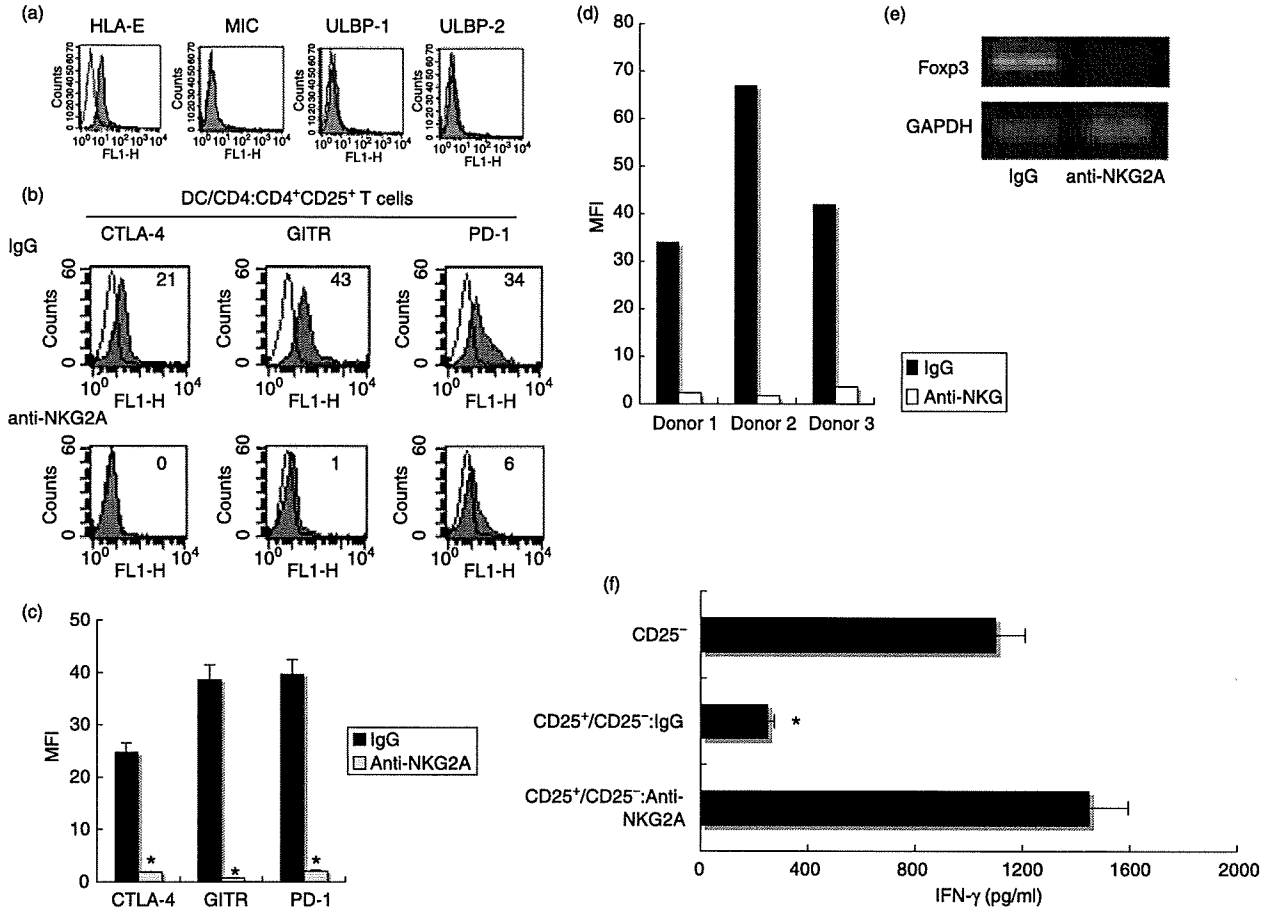

Figure 2. NKG2A signals of natural killer (NK) cells are required for the dendritic cell (DC) induction of $CD4^+$ $CD25^+$ T cells with the regulatory phenotype. (a) Surface expression of the ligands of NKG2A (HLA-E) as well as NKG2D (MIC, ULBP1 and ULBP2) in human non-transformed hepatocytes (NHs) were assessed by flow cytometry (closed histograms). Open histograms show isotype control staining. (b, c) Interleukin (IL)-2-preactivated NK cells were co-cultured with NHs in the presence of 30 μg/ml of anti-NKG2A neutralizing antibody (Ab) (anti-NKG2A) or control IgG. DCs (1×10^5) were then stimulated with the supernatant obtained from the co-cultured medium for 24 hr. After washing three times, DCs were cultured with allogeneic $CD4^+$ T cells for 48 hr. $CD4^+$ $CD25^+$ cells isolated from the co-culture were subjected to FCM for their surface expression of cytotoxic T lymphocyte antigen-4 (CTLA-4), glucocorticoid-induced TNF receptor (GITR) and programmed death-1 (PD-1) (closed histograms). Open histograms show isotype control staining. Numbers on the upper right indicate the mean fluorescence intensity (MFI) of each type of stained cell. All experiments were performed three times. Representative data (b) and composite results with statistical analysis (c) are shown as the MFI of the staining cells. $^*P < 0{\cdot}05$ vs. responses of IgG group. The experiment was performed in different set of donors and similar results were obtained. (d) The inhibitory effect of anti-NKG2A Ab on PD-1 expression of $CD4^+$ $CD25^+$ T cells stimulated with allogeneic DCs from three different donors. Data are shown as MFI. (e) $CD4^+$ $CD25^+$ T cells were stimulated and purified as described above. The mRNA expression of Foxp3 and GAPDH (glyceraldehyde 3-phosphate dehydrogenase) was examined by reverse transcription-polymerase chain reaction (RT-PCR. (f) $CD4^+$ $CD25^+$ T cells (1×10^5/well) isolated from DC and $CD4^+$ T cell co-cultures were cultured with freshly isolated autologous $CD4^+$ $CD25^-$ T cells at a ratio of 1 : 1 in the presence of plate-bound anti-CD3 Ab ($CD25^+/CD25^-$). The anti-CD3 Ab-activated $CD4^+$ $CD25^-$ T cells alone were used as a positive control ($CD25^-$). Interferon (IFN)-γ was measured for each supernatant obtained after 48 hr of co-culture by enzyme-linked immunosorbent assay (ELISA). $^*P < 0{\cdot}05$. All experiments were performed three times; representative results are shown.

Suppressive actions of $CD4^+$ $CD25^+$ Treg cells, induced by NH/IL-2 NK-primed DCs, depends on PD-1-mediated negative costimulatory signals

The suppressive activities of $CD4^+$ $CD25^+$ Treg cells reportedly depend on various kinds of mediators, such as CTLA-4, IL-10 and/or TGF-β, but the exact mechanisms of the actions have not been fully elucidated.[1,6,12–14] PD-1, recently identified as a negative costimulatory receptor of the B-7 family, is expressed in $CD4^+$ $CD25^+$ Treg cells, indicating that PD-1-mediated negative signals may be involved in the regulatory functions of $CD4^+$ $CD25^+$ Treg cells.[9] Thus, we evaluated the involvement of these molecules in the suppressive activities of $CD4^+$ $CD25^+$ Treg cells. For this purpose, the blocking Ab of CTLA-4, GITR, PD-1, TGF-β or IL-10 was added

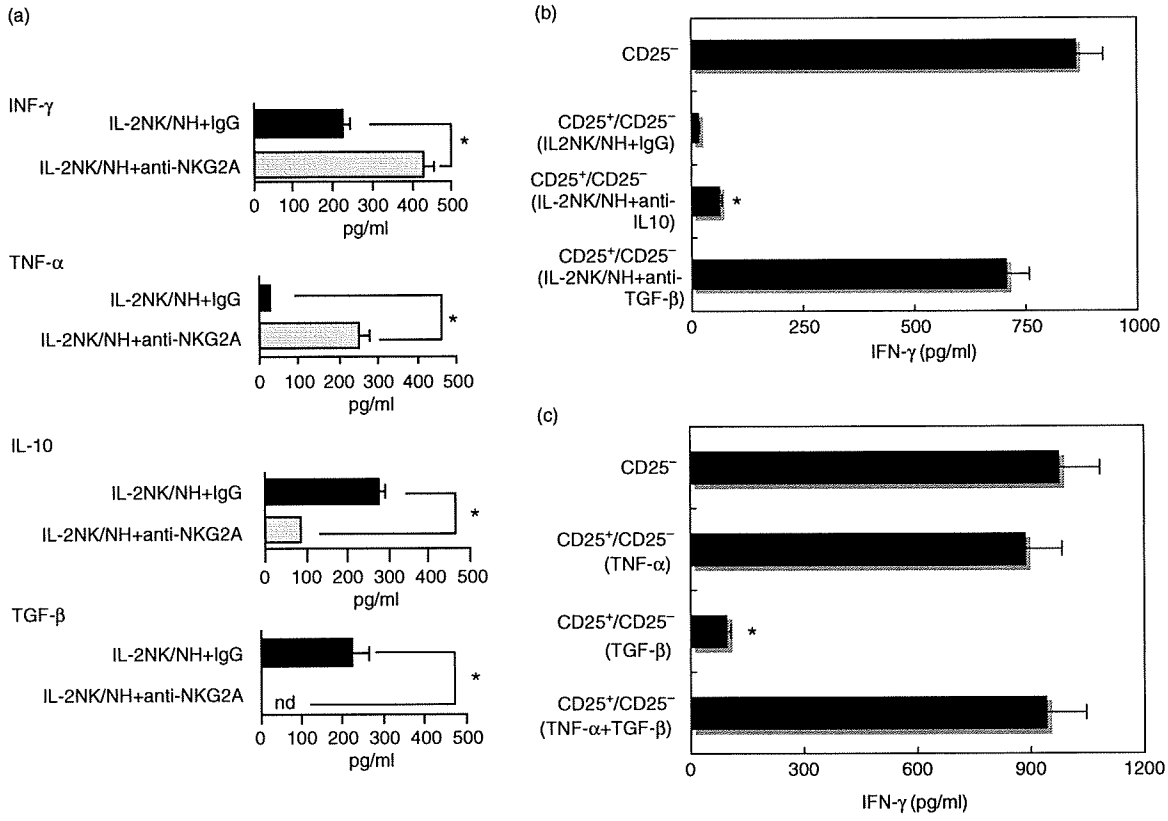

Figure 3. Change of cytokine production pattern of natural killer (NK) cells through NKG2A signals is responsible for the dendritic cell (DC) induction of $CD4^+$ $CD25^+$ Treg cells. (a) NK cells prestimulated with interleukin (IL)-2 were cultured with human non-transformed hepatocytes (NHs) in the presence of masking antibodies (Abs) of NKG2A (IL-2 NK/NH + anti-NKG2A) or isotype control IgG (IL-2 NK/NH + IgG) for 24 hr. *$P < 0{\cdot}05$. (b) IL-2 activated NK cells were co-cultured with NHs (IL-2 NK/NH). DCs (1×10^5) were stimulated with the culture supernatant in the presence of anti-IL-10, anti-transforming growth factor (TGF)-β neutralizing Ab or control IgG for 24 hr. DCs were washed thoroughly and co-cultured with allogeneic $CD4^+$ T cells for 48 hr. Next, the isolated $CD4^+$ $CD25^+$ T cells (1×10^5/well) were co-cultured with autologous $CD4^+$ $CD25^-$ T cells in the presence of plate-bound anti-CD3 Ab at a ratio of 1 : 1. Interferon (IFN)-γ production from the culture supernatant was examined by enzyme-linked immunosorbent assay. *$P < 0{\cdot}05$ vs. responses of anti-CD3 Ab-stimulated $CD4^+$ $CD25^-$ T cells. (c) DCs (1×10^5) were stimulated with 50 ng/ml TNF-α, 100 ng/ml TGF-β or both for 24 hr. After thorough washing, they were co-cultured with allogeneic $CD4^+$ T cells for 48 hr. $CD4^+$ $CD25^+$ T cells (1×10^5/well) were isolated from the DC and $CD4^+$ co-cultures and cultured with freshly isolated autologous $CD4^+$ $CD25^-$ T cells at a ratio of 1 : 1 in the presence of plate-bound anti-CD3 Ab. IFN-γ production was examined as described above. *$P < 0{\cdot}05$ vs. responses of anti-CD3 Ab-stimulated $CD4^+$ $CD25^-$ T cells.

during co-cultures of $CD4^+$ $CD25^+$/$CD4^+$ $CD25^-$ T cells in the presence of anti-CD3 Ab. In case of natural $CD4^+$ $CD25^+$ T cells, their suppressive action was partially reversed on addition of anti-CTLA-4 Ab. By contrast, they preserved their suppressive capacity even in the presence of the blocking Ab of GITR, PD-1, TGF-β or IL-10 (Fig. 4a). When $CD4^+$ $CD25^+$ Treg cells induced by NH/IL-2 NK-primed DCs were used instead of natural $CD4^+$ $CD25^+$ T cells, their suppressive activity was markedly reduced on addition of the blocking Ab of PD-1 but not CTLA-4, IL-10, TGF-β or GITR (Fig. 4a). The regulatory functions of these Treg cells were required for direct cell-to-cell contact because separation of $CD4^+$ $CD25^+$ Treg cells and $CD4^+$ $CD25^-$ T cells in transwell chambers virtually abolished their suppressive effects (data not shown). We also confirmed the presence of PDL-1 expression on $CD4^+$ $CD25^-$ T cells when they were activated with anti-CD3 Ab (Fig. 4b), suggesting that effector cells themselves induce suppressive activities of $CD4^+$ $CD25^+$ Treg cells. Taken together, these results further reinforced the hypothesis that $CD4^+$ $CD25^+$ Treg cells induced by NH/IL-2 NK-primed DCs were different from natural $CD4^+$ $CD25^+$ Treg cells in their PD-1-dependent suppressive functions.

Discussion

Recent studies have revealed that activated NK cells positively regulate DC activation and maturation either through direct contact via NK cell receptors (NKp30, NKG2D, etc.) or in co-ordination with various kinds of cytokines (IFN-γ, TNF-α, etc.).[15–18] However, the issue of

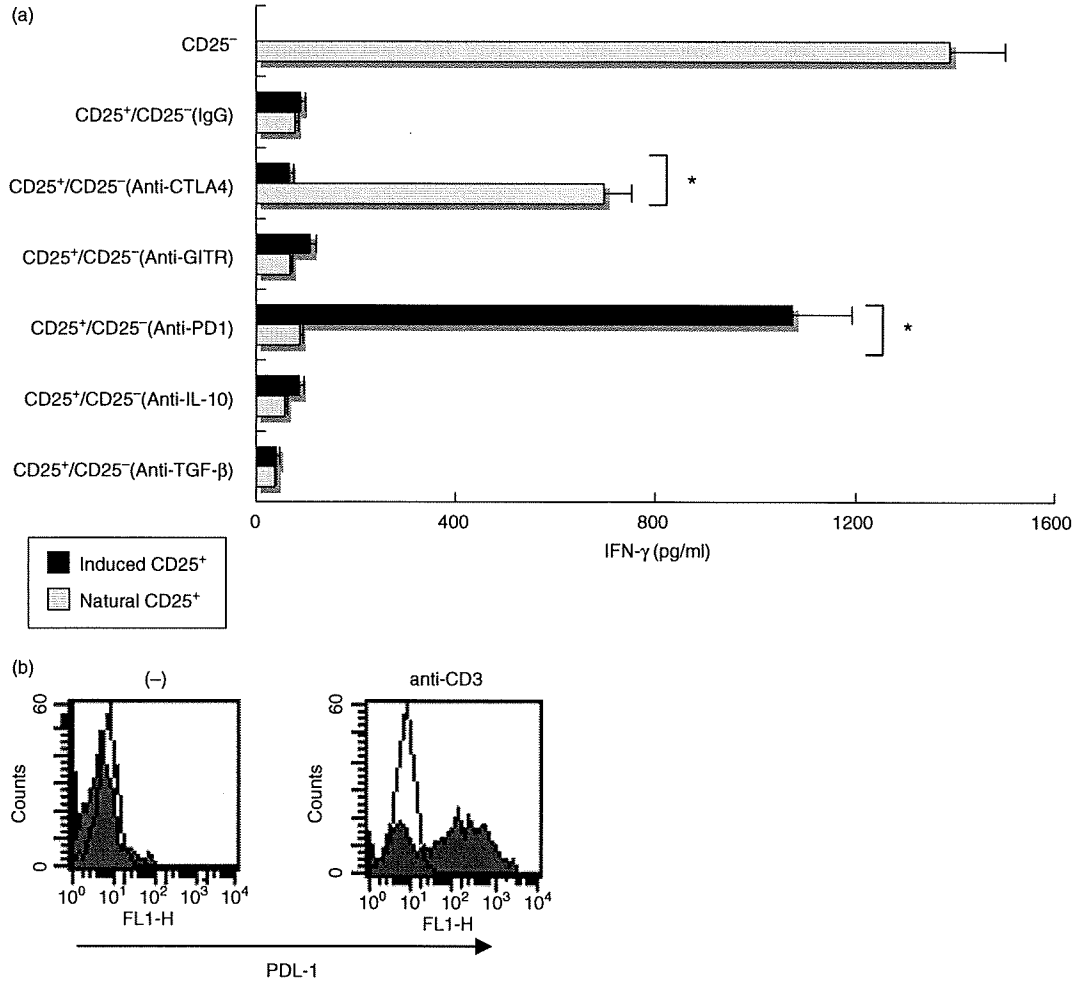

Figure 4. $CD4^+$ $CD25^+$ Treg cells induced by interleukin (IL)-2 natural killer (NK)/human non-transformed hepatocytes (NH)-treated dendritic cell (DC) suppressed T cell activation through programmed death-1 (PD-1)/programmed death ligand-1 (PDL-1) interactions. (a) DCs (1×10^5) were stimulated with the IL-2 NK/NH supernatant for 24 hr, and then cultured with allogeneic $CD4^+$ T cells for 48 hr. $CD4^+$ $CD25^+$ fractions were isolated from the DC/$CD4^+$ T cell mixtures. Freshly isolated $CD4^+$ $CD25^+$ T cells (natural $CD25^+$) or $CD4^+$ $CD25^+$ T cells induced by NK/NH-primed DCs (induced $CD25^+$) were co-cultured with freshly isolated autologous $CD4^+$ $CD25^-$ T cells at a ratio of 1 : 1 upon stimulation of plate-bound anti-CD3 antibody (Ab). Anti-CTLA-4 (cytotoxic T lymphocyte antigen-4) Ab, anti-GITR (glucocorticoid-induced TNF receptor) Ab, anti-PD-1 Ab, anti-IL-10 Ab, anti-TGF-β Ab or isotype control IgG (20 μg/ml for each) were incubated during $CD4^+$ $CD25^+$/$CD4^+$ $CD25^-$ T cell co-cultures. Interferon (IFN)-γ was measured for each supernatant obtained after 72 hr of co-culture by enzyme-linked immunosorbent assay. $^*P < 0{\cdot}05$ vs. responses of anti-CD3 Ab-stimulated $CD4^+$ $CD25^-$ T cells. (b) Freshly isolated $CD4^+$ $CD25^-$ T cells were incubated with (anti-CD3) or without (–) plate-bound anti-CD3 Ab for 24 hr. PDL-1 expression was assessed by flow cytometry (closed histograms). Open histograms show isotype control staining.

whether NK cells are involved in DC-mediated Treg cell induction has not been resolved. In the present study, we report that the expression of regulatory markers and functions was markedly decreased on $CD4^+$ $CD25^+$ T cells upon exposure to IL-2 NK-primed DCs. By contrast, the interaction of activated NK cells and NH through the NKG2A inhibitory receptor led to DC induction of $CD4^+$ $CD25^+$ T cells with regulatory properties. Furthermore, NKG2A-mediated increase in TGF-β as well as decrease in TNF-α in an NH and NK cell mixture contributed to DC induction of $CD4^+$ $CD25^+$ Treg cells. This is consistent with previous reports showing that TGF-β plays a role in generating the specific DC that activates $CD4^+$ $CD25^+$ Treg cells.[10,11] The findings that TNF-α suppressed TGF-β-mediated priming of DCs to induce Treg cells also extended the previously identified role of TNF-α as a positive regulator of DC activation. In line with our findings, previous reports showed that impairment of $CD4^+$ $CD25^+$ Treg cell activities restored their suppressive functions after blocking TNF-α signals in non-obese diabetic (NOD) mice or in patients with Crohn's disease.[28,29] To our knowledge, the present study is the first description of modulation of NK cells and human hepatocytes through NKG2A-mediated inhibitory

signals that profoundly affect DC functions towards $CD4^+$ $CD25^+$ Treg cells. Because NK cell functions are regulated by the balance between inhibitory and activating signals, any future clarification of the role of other NK inhibitory and activating receptors in DC modulation and Treg cell activation will be of great interest.

The cross-presentation of self-antigens by major histocompatibility complex (MHC) class II pathways constitutes an important step towards generating and/or expanding peripheral Treg cells.[30] However, we initially settled our experimental design by using DCs and Treg cells from different donors, and DCs encountered $CD4^+$ T cells in an 'antigen-free' condition. Therefore, Treg cells induced by NK/NH-primed DCs are generated independently of MHC class II-mediated self-antigen recognition. These results give rise to the possibility that the cross-talk of NK cells, DCs and hepatocytes represents an alternative pathway in the generation and expansion of peripheral Treg cells. However, it should be noted that these results may not apply to all donors because of the complexity of the allogeneic system and the relatively few donors tested.

PD-1-mediated suppressive activities were characteristic for $CD4^+$ $CD25^+$ Treg cells generated by NH/IL-2 NK-primed DCs. By contrast, natural $CD4^+$ $CD25^+$ Treg cells exerted their suppressive function, at least in part, in a CTLA-4-dependent fashion. Recent reports have clarified the existence of two subtypes of Treg cells: natural and inducible $CD4^+$ $CD25^+$ Treg cells. Inducible Treg cells exert suppressive activities by using molecular mechanisms distinct from those of natural regulatory cells.[31] Our findings further identify the novel pathways by which inducible $CD4^+$ $CD25^+$ Treg cell activities triggered by NKG2A inhibitory signals are dependent on PD-1-mediated negative costimulation. A recent report identified the interaction of B7 on effector T cells with costimulatory molecules CD28/CTLA-4 on $CD4^+$ $CD25^+$ Treg cells as molecular mechanisms of their suppressor activity.[32] Thus, it is possible that reverse signalling of PDL-1 on effector cells may also be crucial for the negative costimulator-mediated suppressive action of $CD4^+$ $CD25^+$ Treg cells. In the present study, we did not address the mechanisms by which NH/IL-2 NK-primed DCs induce $CD4^+$ $CD25^+$ Treg cells with PD-1-dependent suppressive functions. Further study will be needed to clarify this issue.

We previously showed that NKG2A is expressed at higher levels from NK cells isolated from peripheral blood in patients with chronic hepatitis C virus (HCV) infection than from those in healthy donors.[20] HCV frequently persists in humans, at least in part, due to inefficient induction of NK activity as well as specific T cell responses.[33–35] The small percentage of patients who spontaneously clear the virus and recover from chronic hepatitis C mount vigorous HCV-specific $CD4^+$ and $CD8^+$ T cell responses.[36,37] Research has described an increased frequency of $CD4^+$ $CD25^+$ T cells in the blood of patients with persistent HCV infection compared with those who have spontaneously cleared HCV.[38,39] Our current findings raise the interesting possibility that increased NKG2A expression on NK cells may lead to DC-mediated induction of Treg cells, leading to the inhibition of adaptive responses to HCV and failure to eliminate this virus. Indeed, $CD4^+$ $CD25^+$ T cells induced by HCV-NK/Hep3B hepatoma cell-primed DCs expressed and suppressed effector T cell functions at greater levels than those induced by N-NK/Hep3B-primed DCs (our unpublished data). Interestingly, a recent study identified PD-1-mediated signals as a critical pathway to induce anergic $CD8^+$ T cells and impair antiviral CTL responses in chronic viral infection.[40] In this regard, the therapeutic modification of the PD-1 pathway may synergistically augment antiviral immunity by suppressing Treg activity and recovering CTL responses. It is important to establish whether the PD-1 pathway in liver lymphocytes may be operable *in vivo* and play a critical role in suppression of virus-specific immunity in HCV infection.

In conclusion, we have demonstrated that interaction of NK cells and hepatic cells via NKG2A leads to DC induction of $CD4^+$ $CD25^+$ T cells with PD-1-dependent regulatory activities. These findings also imply that NK receptor signals of NK cells may dictate DC-mediated adaptive immune responses towards tolerogenic or immunogenic status via induction of Treg cells.

Acknowledgements

This work was supported by a grant-in-aid from the Ministry of Culture, Sports, Science and Technology of Japan and a grant-in-aid for research on hepatitis and BSE from the Ministry of Health, Labour and Welfare of Japan. It was also partially supported by the 21st Century Centre of Excellence Programme of the Ministry of Education, Culture, Sports, Science and Technology of Japan.

References

1 Shevach EM. $CD4^+$ $CD25^+$ suppressor T cells: more questions than answers. *Nat Rev Immunol* 2002; **2**:389–400.

2 Jonuleit H, Schmitt E, Stassen M, Tuettenberg A, Knop J, Enk AH. Identification of functional characterization of human $CD4^+$ $CD25^+$ T cells with regulatory properties isolated from peripheral blood. *J Exp Med* 2001; **193**:1285–94.

3 Dieckmann D, Plottner H, Berchtold S, Berger T, Schuler G. *Ex vivo* isolation and characterization of $CD4^+$ $CD25^+$ T cells with regulatory properties from human blood. *J Exp Med* 2001; **193**:1303–10.

4 Belkald Y, Piccirillo CA, Mendez S, Shevach EM, Sacks DL. $CD4^+$ $CD25^+$ regulatory T cells control Leishmania major persistence and immunity. *Nature* 2002; **420**:502–7.

5 Wang HY, Lee DA, Peng G, Guo Z, Li Y, Kiniwa Y, Shevach EM, Wang RF. Tumour-specific human $CD4^+$ regulatory T cells

and their ligands: implication for immunotherapy. *Immunity* 2004; **20**:107–18.

6 Read S, Malmstrom V, Powrie F. Cytotoxic T lymphocyte-associated antigen 4 plays an essential role in the function of $CD4^+$ $CD25^+$ regulatory cells that control intestinal inflammation. *J Exp Med* 2002; **192**:295–302.

7 Herman AE, Freeman GJ, Mathis D, Benoist C. $CD4^+$ $CD25^+$ T regulatory cells dependent on ICOS promote regulation of effector cells in the prediabetic lesion. *J Exp Med* 2004; **199**:1479–89.

8 Khoury SJ, Sayegh MH. The roles of the new negative T cell costimulatory pathways in regulating autoimmunity. *Immunity* 2004; **20**:529–38.

9 Gavin MA, Clarke SR, Negrou E, Gallegos A, Rudensky A. Homeostasis and anergy of CD4 ($^+$) CD25 ($^+$) suppressor T cells *in vivo*. *Nat Immunol* 2004; **3**:33–41.

10 Steinman RM, Hawiger D, Nussenzweig D. Tolerogenic dendritic cells. *Annu Rev Immunol* 2003; **21**:685–711.

11 Mahnke K, Quan Y, Knop J, Enk AH. Induction of $CD4^+$ $CD25^+$ regulatory T cells by targeting of antigens to immature dendritic cells. *Blood* 2003; **101**:4862–9.

12 Annacker O, Pimenta-Araujo R, Burlen-Defranoux O, Barbosa TC, Cumano A, Bandeira A. $CD4^+$ $CD25^+$ T cells regulate the expansion of peripheral $CD4^+$ T cells through the production of IL-10. *J Immunol* 2001; **166**:3008–18.

13 Yamagiwa S, Gray JD, Hashimoto H, Horwitz DA. A role of TGF-β in the generation and expansion of $CD4^+$ $CD25^+$ regulatory T cells from human peripheral blood. *J Immunol* 2001; **166**:7282–9.

14 Peng Y, Laouar Y, Li MO, Green EA, Flavell RA. TGF-β regulates *in vivo* expansion of Foxp3-expressing $CD4^+$ $CD25^+$ regulatory T cells responsible for protection against diabetes. *Proc Natl Acad Sci USA* 2004; **101**:4572–7.

15 Moretta A. The dialogue between human natural killer cells and dendritic cells. *Curr Opin Immunol* 2005; **17**:306–11.

16 Walzer T, Dalod M, Robbins SH, Zitvogel L, Vivier E. Natural killer cells and dendritic cells: 'L'union fait la force'. *Blood* 2005; **106**:2252–8.

17 Mocikat R, Braumuller H, Gumy A *et al.* Natural killer cells activated by MHC^{LOW} targets prime dendritic cells to induce protective CD8 T cell responses. *Immunity* 2003; **19**:561–9.

18 Van den Broeke LT, Daschbach E, Thomas EK, Andringa G, Berzofsky JA. Dendritic cell-induced activation of adaptive and innate antitumour immunity. *J Immunol* 2003; **171**:5842–52.

19 Cerwenka A, Lanier LL. Natural killer cells, viruses and cancer. *Nat Rev Immunol* 2001; **1**:41–9.

20 Jinushi M, Takehara T, Tatsumi T *et al.* Negative regulation of NK cell activities by inhibitory receptor CD94/NKG2A leads to the altered NK cell-induced modulation of dendritic cell functions in chronic hepatitis C virus infection. *J Immunol* 2004; **173**:6072–81.

21 Lee N, Goodlett DR, Ishitani A, Marquardt H, Geraghty DE. HLA-E surface expression depends on binding of TAP-dependent peptides derived from certain HLA class I signal sequences. *J Immunol* 1998; **160**:4951–60.

22 Bauer S, Groh V, Wu J, Steinle A, Phillips JH, Lanier LL, Spies T. Activation of NK cells and T cells by NKG2D, a receptor for stress-inducible MICA. *Science* 1999; **285**:727–9.

23 Pende D, Sivori S, Accame L *et al.* HLA-G recognition by human natural killer cells. Involvement of CD94 both as inhibitory and as activating receptor complex. *Eur J Immunol* 1997; **27**:1875–80.

24 Valerie V, Vosters O, Beuneu C, Nicaise C, Stordeur P, Goldman M. Induction of FOXP3-expressing regulatory $CD4^+$ T cells by human mature autologous dendritic cells. *Eur J Immunol* 2003; **34**:762–72.

25 Shimizu J, Yamazaki S, Takahashi T, Ishida Y, Sakaguchi S. Stimulation of $CD4^+$ $CD25^+$ regulatory T cells through GITR break immunological self-tolerance. *Nat Immunol* 2002; **3**:135–42.

26 Hori S, Nomura T, Sakaguchi S. Control of regulatory T cell development by the transcription factor Foxp3. *Science* 2003; **299**:1057–61.

27 Piccioli D, Sbrana S, Melandri E, Valiante NM. Contact-dependent stimulation and inhibition of dendritic cells by natural killer cells. *J Exp Med* 2002; **195**:335–41.

28 Ehrenstein MR, Evans JG, Singh A, Moore S, Warnes G, Isenberg DA, Mauri C. Compromised function of regulatory T cells in rheumatoid arthritis and reversal by anti-TNF-α therapy. *J Exp Med* 2004; **200**:277–85.

29 Wu AJ, Hua H, Munson SH, McDevitt HO. Tumour necrosis factor-α regulation of $CD4^+$ $CD25^+$ T cell levels in NOD mice. *Proc Natl Acad Sci USA* 2002; **99**:12287–92.

30 Kretschmer K, Apostolou I, Hawiger D, Khazaie K, Nussenzweig MC, von Boehmer H. Inducing and expanding regulatory T cell populations by foreign antigen. *Nat Immunol* 2005; **6**:1219–27.

31 Bluestone JA, Abbas AK. Natural and adaptive regulatory T cells. *Nat Rev Immunol* 2003; **3**:253–7.

32 Paust S, Lu L, McCarty N, Cantor H. Engagement of B7 on effector T cells by regulatory T cells prevents autoimmune disease. *Proc Natl Acad Sci USA* 2004; **101**:10398–403.

33 Ahmad A, Alvarez F. Role of NK and NKT cells in the immunopathogenesis of HCV-induced hepatitis. *J Leukoc Biol* 2004; **76**:743–59.

34 Golden-Mason L, Rosen HR. Natural killer cells: primary target for hepatitis C virus immune evasion strategies. *Liver Transplant* 2006; **12**:363–72.

35 Rehermann B, Nascimbeni M. Immunology of hepatitis B virus and hepatitis C virus infection. *Nat Rev Immunol* 2005; **5**:215–29.

36 Lauer GM, Barnes E, Lucas M *et al.* High resolution analysis of cellular immune responses in resolved and persistent hepatitis C virus infection. *Gastroenterology* 2004; **127**:924–36.

37 Cox AL, Mosbruger T, Lauer GM, Pardoll D, Thomas DL, Ray S. Comprehensive analysis of $CD8^+$ T cell responses during longitudinal study of acute human hepatitis C. *Hepatology* 2005; **42**:104–12.

38 Cabrera R, Tu Z, Xu Y, Firpi RJ, Rosen HR, Liu C, Nelson DR. An immunomodulatory role for $CD4^+$ $CD25^+$ regulatory T lymphocytes in hepatitis C virus infection. *Hepatology* 2004; **40**:1062–71.

39 Rushbrook SM, Ward SM, Unitt E, Vowler M, Lucas M, Kleneman P, Alexander GJ. Regulatory T cells suppress *in vitro* proliferation of virus-specific $CD8^+$ T cells during persistent hepatitis C virus infection. *J Virol* 2005; **79**:7852–9.

40 Barber DL, Wherry EJ, Masopust D, Zhu B, Allison JP, Freeman GJ, Ahmed R. Restoring function in exhausted CD8 T cells during chronic viral infection. *Nature* 2006; **439**:682–7.

J Gastroenterol
DOI 10.1007/s00535-009-0160-5

ORIGINAL ARTICLE—LIVER, PANCREAS, AND BILIARY TRACT

The complement component C3a fragment is a potential biomarker for hepatitis C virus-related hepatocellular carcinoma

Shuji Kanmura · Hirofumi Uto · Yuko Sato · Koutarou Kumagai · Fumisato Sasaki · Akihiro Moriuchi · Makoto Oketani · Akio Ido · Kenji Nagata · Katsuhiro Hayashi · Sherri O. Stuver · Hirohito Tsubouchi

Received: 1 July 2009 / Accepted: 28 October 2009

Abstract
Background Hepatocellular carcinoma (HCC) has a high mortality rate, and early detection of HCC improves patient survival. However, the molecular diagnostic markers for early HCC have not been fully elucidated. The aim of this study was to identify novel diagnostic markers for HCC.
Methods Serum protein profiles of 45 hepatitis C virus infection (HCV)-related HCC patients (HCV-HCC) were compared to 42 HCV-related chronic liver disease patients without HCC (HCV-CLD) and 21 healthy volunteers using the ProteinChip SELDI system. One of the identified proteins was evaluated as a diagnostic marker for HCC in patients with HCV.
Results Five protein peaks (4067, 4470, 7564, 7929, and 8130 m/z) had p-values less than 1×10^{-7} and were significantly increased in the sera of HCV-HCC patients compared to HCV-CLD patients and healthy volunteers. Among these proteins, an 8130 m/z peak was the most differentially expressed and identified as the complement component 3a (C3a) fragment. For HCV-HCC and HCV-CLD, the relative intensity of this C3a fragment had the best area under the ROC curve [0.70], followed by des-γ-carboxy prothrombin (DCP) [0.68], lectin-bound alpha fetoprotein (AFP-L3) [0.58] and AFP [0.53] for HCC. A combined analysis of the C3a fragment, AFP and DCP led to a 98% positive identification rate. In addition, the measurable C3a fragment in some HCC patients was not only significantly higher in the year of HCC onset compared to the pre-onset year, but also decreased after treatment.
Conclusions The 8130 m/z C3a fragment is a potential marker for the early detection of HCV-related HCC.

Keywords Hepatocellular carcinoma · Complement component C3a · Serum proteomics · Serum biomarkers · Proteinchip SELDI system · Hepatitis C virus

S. Kanmura · H. Uto (✉) · K. Kumagai · F. Sasaki · A. Moriuchi · M. Oketani · A. Ido · H. Tsubouchi
Digestive Disease and Life-style Related Disease Health Research, Human and Environmental Sciences, Kagoshima University Graduate School of Medical and Dental Sciences, 8-35-1 Sakuragaoka, Kagoshima 890-8520, Japan
e-mail: hirouto@m2.kufm.kagoshima-u.ac.jp

Y. Sato
Miyazaki Prefectual Industrial Support Foundation, Miyazaki, Japan

K. Nagata
Division of Gastroenterology and Hematology, Internal Medicine, Faculty of Medicine, University of Miyazaki, Miyazaki, Japan

K. Hayashi
Faculty of Medicine, Center for Medical Education, University of Miyazaki, Miyazaki, Japan

S. O. Stuver
Department of Epidemiology, Boston University School of Public Health, Boston, MA, USA

S. O. Stuver
Department of Epidemiology, Harvard School of Public Health, Boston, MA, USA

Introduction

Hepatocellular carcinoma (HCC) is reportedly the third most frequent cause of global cancer-related deaths, and the incidence of HCC is increasing worldwide [1, 2]. The clearly established risk factor for HCC is chronic hepatitis C virus (HCV) infection [3].

Published online: 09 December 2009

To date, both ultrasonography and serum tumor markers such as the alpha fetoprotein (AFP), and des-γ-carboxy prothrombin (DCP) assay are the principle methods for screening and detecting HCC. Routine screening is the best method to detect early HCC and improve patient survival; however, elevated serum AFP and DCP levels have insufficient sensitivity and specificity, respectively. The sensitivity and specificity of serum elevated AFP levels were reported to range from 39–64% and 76–91%, while those of the serum elevated DCP levels were 41–77% and 72–98%, respectively [4–9]. In addition, it was recently reported that only a small percentage of small HCC tumors were diagnosed based on AFP and DCP [6, 10]. The lens culinaris agglutinin-reactive fraction of AFP (lectin-bound AFP or AFP-L3) has been reported to be elevated in the serum of HCC patients. Although AFP-L3 has a high range of specificity for detecting HCC, the sensitivity is low [11, 12]. The ability to detect early HCC, prior to the onset of clinical symptoms, leads to curative treatment and significantly improves the disease prognosis. Thus, additional biochemical markers are necessary for the specific detection of early HCC.

Serum profiling using a proteomic approach is thought to be a useful technique to detect or predict early HCC in chronic liver disease patients. Studies using the ProteinChip SELDI system, which is a powerful tool to discover new biomarkers, have shown that this method may be successfully used to diagnose HCC. Zinkin et al. [13], Schwegler et al. [14] and our research group [15] previously detected early HCC using the profile of several protein peaks that were identified by the ProteinChip SELDI system. Paradis et al. [16] reported the highest discriminating peak (8900 Da), which was identified as the V10 fragment of vitronectin. Furthermore, Lee et al. [17] described complement 3a, which had a molecular weight of approximately 8900 Da, as a novel marker of HCC. Therefore, using this proteomic approach to identify specific proteins may not only help establish simple methods to detect HCC, but also further our understanding of the molecular mechanisms of hepatocarcinogenesis and facilitate the development of novel cancer therapies. Therefore, this study assessed and compared the protein expression profiles in the sera of HCC patients in order to identify a more useful biomarker of HCC-associated HCV infection using proteomic approach.

Materials and methods

Samples

Eighty-seven patients [45 HCC patients and 42 patients with chronic liver diseases without HCC (CLD)] with HCV infection were selected to participate in this study (Table 1). These patients provided informed consent. Serum samples were collected by the Faculty of Medicine, University of Miyazaki (Miyazaki, Japan), and some patients were in a hyperendemic HCV area with a cohort study in Miyazaki [18]. The sera of all patients with and without HCC, which was confirmed by abdominal ultrasonography or computed tomography, were obtained prior to treatment. All of the sera samples from HCV-infected patients were analyzed in a previous study [15]. In addition, sera from 10 HCV-HCC patients who were diagnosed with HCC within 1 or 2 years and sera from five patients who had received radiofrequency ablation (RFA), percutaneous ethanol injection therapy (PEIT) and/or transarterial chemoembolization (TACE) for HCC were collected through a cohort study in Miyazaki. We also analyzed the sera of 21 healthy volunteers without HCC as controls. After freezing and thawing once, all samples were separated into 50–100 μl aliquots and refrozen at −80°C. The study protocol was approved by the Ethics Committee of the Faculty of Medicine, University of Miyazaki, Kagoshima University Graduate School of Medical and Dental Sciences, and Harvard School of Public Health and Boston University School of Public Health.

Table 1 Patient characteristics

	HCC[a]	CLD[b]	*p* value
Patients (male/female)	45 (40/5)	42 (40/2)	–
Age	73.6 [63–85]	61.8 [41–83]	<0.0001
PLT[c] ($\times 10^4$/ul)	12.5 ± 5.8	8.4 ± 4.6	0.001
Albumin (g/dl)	3.8 ± 0.8	4.2 ± 1.6	0.8
ALT[d] (IU/l)	57.7 ± 28.3	52.8 ± 37.5	0.7
AFP[e] (ng/ml)	311 ± 1144	51.6 ± 36.1 (38)	0.008
DCP[f] (mAU/ml)	235 ± 605 (44)	37.1 ± 59.8 (39)	<0.0001
HA[g] (ng/ml)	388 ± 446 (40)	280 ± 272 (27)	0.6
Diameter of HCC (mm)	23.2 [10–40]	–	–
TNM stage[h] (I/II/III/IV)	24/18/3/0	–	–

Data are shown as the means ± SD or means [range] (numbers)

[a] Hepatocellular carcinoma

[b] Chronic liver disease

[c] Platelet counts

[d] Alanine aminotransferase

[e] Alpha fetoprotein

[f] Des-γ-carboxy prothrombin

[g] Hyaluronic acid

[h] TNM; primary tumor/lymph node/distant metastasis

SELDI-TOF/MS analysis of sera

Expression difference mapping analysis profiles of the samples were obtained using weak cation-exchange (CM10) ProteinChip Arrays (Bio-Rad Laboratories). Arrays were analyzed by ProteinChip reader as previously reported [15]. In addition, the laser intensity ranged from 220 to 245, with a detector sensitivity of 8, and spectra ranging from 1300 to 150000 m/z were selected for analysis in this study.

Separation of candidate biomarker (8.1 k m/z)

The purification strategy was determined by the ProteinChip Arrays. Two hundred microliters of sera from HCV-HCC patients were diluted 5-fold into 50 mM Na-phosphate buffer, pH 7.0, and loaded onto a CM-Ceramic HyperD F spin column (Bio-Rad Laboratories). After equilibrating with the same buffer, the samples were eluted with a stepwise sodium chloride gradient from 0, 200, 300, and 1000 mM. The elution was desalinated and concentrated using a centrifugal concentrator (VIVA-SPIN, Vivascience, Hannover, Germany), and the purification progress was monitored using NP20 arrays. The flow-through fraction was dialyzed and then separated by 16.5% tricine one-dimensional sodium dodecyl sulfate–polyacrylamide gel electrophoresis (SDS–PAGE). The SDS–PAGE samples were run in tricine sodium dodecyl sulfate buffer according to the manufacturer's instructions and then stained with Coomassie brilliant blue (CBB).

Identification of the candidate biomarker (8.1 k m/z)

Gel pieces containing the target 8.1 k m/z protein were excised. The excised bands were reduced and alkylated for 30 min at room temperature, and then digested with trypsin (Modified Sequence Grade, Roche Diagnostics, Basel, Switzerland) in Tris–HCl, pH 8.0, for 20 h at 35°. The reaction solution was applied to NP20 arrays and allowed to air dry. To identify the protein, the digested peptides were purified by high-performance liquid chromatography (HPLC; MAGIC 2002; Michrom Bioresources Inc., Auburn, CA) and analyzed by Q-Tof2 (Micromass; Waters Ltd., Hertsfordshire, UK). The HPLC solvent consisted of solvent A (2% acetonitlile/0.1% formic acid) and B (90% acetonitlile/0.1% formic acid). The digested peptides were separated with a linear gradient from 10 to 50% solvent B with a flow rate of 400 nl/min using HPLC [19]. Mass spectral data were searched with Mascot (http://www.matrixscience.com) to identify proteins based on the peptide mass [20, 21].

Immunodepletion assay

For immunodepletion, serum samples were prepared as follows. Sera (250 μl) from HCC patients were diluted 5-fold in 50 mM Tris–HCl buffer, pH 8.0, and loaded onto a CM-Sepharose Fast Flow spin column (GE Healthcare Bio-Sciences Corp., NJ). After equilibration with the same buffer, the samples were eluted with a stepwise sodium chloride gradient from 0, 500, and 1000 mM. The elution from each NaCl concentration was monitored using NP20 arrays. To prepare the antibodies for immunodepletion, 6 μl anti-human C3 antibody, which detected C3 and C3a expression, or anti-C4a antibody (Santa Cruz Biotechnology, Santa Cruz, CA) was incubated with 20 μl Interaction Discovery Mapping (IDM) affinity beads (Bio-Rad Laboratories) and Protein A (Sigma Chemical Co, St. Louis, MO) over night at 4° with shaking. These beads were centrifuged, and the supernatant was discarded. The beads were washed with 50 mM phosphate buffer (pH 7.0), and 3 μl of the prepared serum sample was incubated with 15 μl IDM affinity beads with shaking for 2 h at 4°. As a negative control, 3 μl sample was incubated with IDM affinity beads and Protein A with an anti-C4a antibody or without antibody. After the incubation, the samples were cleared by centrifugation, and 5 μl of each supernatant was analyzed on NP20 ProteinChip arrays in a PBS II reader.

Cell culture and SELDI-TOF/MS analysis of culture supernatants

The human hepatocarcinoma cell line HuH-7 and human hepatoblastoma cell line HepG2 were cultured in Dulbecco's modified Eagle's medium supplemented with 10% fetal bovine serum (FBS), 100 IU/ml penicillin G, and 100 mg/ml streptomycin sulfate (Invitrogen, Carlsbad, CA). Before starting the experiments, the cells were cultured on 96-well microplates in medium without FBS for 24 h. After washing with FBS-free media, the cells were cultured for 24 h with FBS-free media with or without 500 μg/ml of C3a (Calbiochem, San Diego, CA). The supernatants were collected by centrifugation and analyzed for the expression of 8.1 k m/z using the ProteinChip system.

Statistical analysis

Values are shown as the means ± SD. Statistical differences, including laboratory data and individual peaks in SELDI TOF/MS, were determined using the Mann–Whitney U test. Values of $p < 0.05$ were considered statistically significant. The discriminatory power for each putative marker was described via receiver operating characteristics

(ROC) area under the curve (AUC). These statistical analyses were performed using STATVIEW 4.5 software (Abacus Concepts, Berkeley, CA), SPSS software (SPSS Inc., Chicago, IL), JMP software, or Ciphergen ProteinChip Software, version 3.0.2.

Results

Profiling sera from HCC patients and healthy controls

We analyzed the sera of all patients with HCV-HCC or HCV-CLD and healthy controls without HCC using the CM10 ProteinChip array to identity the most differential protein peak. Peaks were automatically detected using the Ciphergen ProteinChip Software 3.0.2. following baseline subtraction as described previously [15, 22]. This analysis identified 178 protein peak clusters, as seen in the spectrum representations from the three groups (HCV-HCC, HCV-CLD, and healthy control) in the 3000- to 15000-m/z range. Peak expressions were increased for 18 proteins and decreased for 14 proteins in sera from HCV-HCC patients compared to HCV-CLD patients. Compared to healthy subjects, 68 protein peaks were increased, and 16 protein peak intensities were decreased in the sera of HCV-HCC patients. Five protein peaks (4067, 4470, 7564, 7929, and 8130 m/z) had a p-value less than 1×10^{-7} and were significantly increased in the sera of HCC patients compared to the sera of HCV-CLD patients and healthy volunteers. In particular, an 8130 m/z peak was the most significantly different peak and had the most differential expression profile between patients with HCV-HCC and with HCV-CLD.

Purification and identification of the 8.1 k m/z peak

We optimized the adsorption and desorption conditions on the arrays using an HCV-HCC patient serum sample and healthy volunteer serum sample in order to determine a procedure to purify the target 8.1 k m/z protein. The optimal pH for retention of the 8.1 k m/z protein was a *pI* value of approximately 7.0 on the CM10 arrays, which indicates that weak cation-exchange sorbents and buffer pH should be fixed for further experiments. The target protein was eluted by increasing the sodium chloride concentrations in a Na-phosphate buffer and was eluted in the 1000 mM sodium chloride fraction. The concentrated serum protein that was eluted with 1000 mM sodium chloride was applied to SDS–PAGE for further separation. The 8.1 k m/z protein was identified and excised by in-gel trypsin digestion for identification. The peptide sequences were analyzed using liquid chromatography (LC)-MS/MS and then examined by a database search with Mascot. The digested peptides matched human complement C3a (Fig. 1).

After reacting the HCC sera with anti-complement C3a or anti-C4 antibodies or without antibody, the supernatants were analyzed by the SELDI ProteinChip system for immunodepletion. Analysis of the supernatant showed that only the 8.1 k m/z peak corresponding to complement C3a

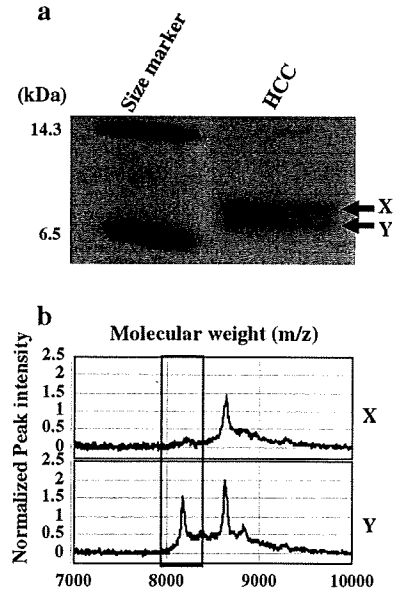

c Complement component 3:
Total score: 70, Peptides matched: 2

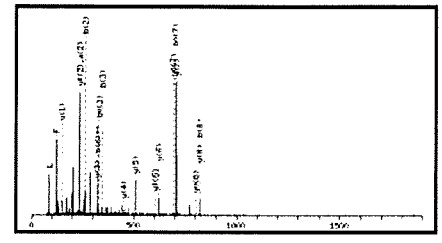

FISLGEACK , Start – End Sequence: 713 - 721

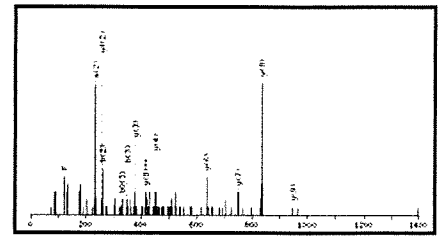

FISLGEACKK , Start – End Sequence: 713 - 722

Fig. 1 **a** Partially purified proteins were separated by SDS–PAGE using serum samples from HCV-HCC patients. The Coomassie-stained SDS-PAGE gel shows two clear bands at approximately 8 kDa (*X* and *Y*). **b** After each band (*X* and *Y*) was excised from the gel, the proteins were extracted and analyzed using the ProteinChip system. The target protein in the excised band was detected, and the 8.1 k m/z peak corresponded only to the "*Y*" band contained in gel. **c** The excised "*Y*" band was alkylated and digested using trypsin. The peptides were collected and subjected to LC–MS/MS analysis. The proteins, which were derived from complement C3a, were identified using a database search

was reduced. On the other hand, immunodepletion with a control anti-C4 antibody or without antibody did not reduce the 8.1 k m/z peak (Fig. 2).

Profiling the C3a of sera from patients with HCC and without HCC

The 8.1 k m/z peak was confirmed as the complement C3a fragment using an immunodepletion assay. However, C3a was stabilized as C3adesArg with a molecular weight of approximately 8.9 k m/z. Figure 3a, b compares the expression of the 8.1 k m/z peak in the sera of HCV-HCC or HCV-CLD patients and healthy controls. The intensities

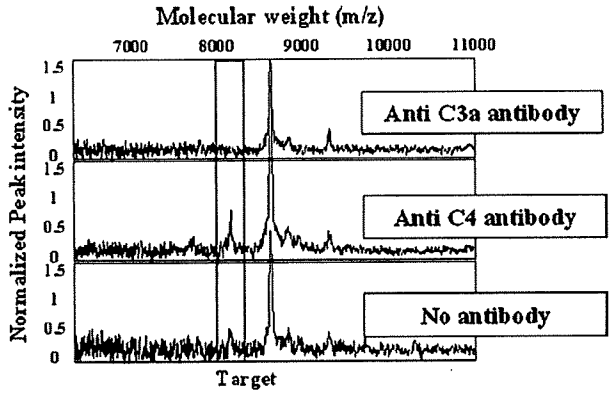

Fig. 2 Immunodepletion assay of the C3a fragment. Analysis of supernatant that had been immunodepleted with an anti-C3a antibody showed that only the 8.1 k m/z peak corresponding to complement C3a was reduced. Supernatants that had been immunodepleted with either a control anti-C4 antibody or without antibody did not have reduced 8.1 k m/z peaks by the ProteinChip system

in HCC patient sera were significantly higher than those in the HCV-CLD patients or healthy controls. The expression of the 8.9 k m/z peak in HCV-HCC patients was also higher than that in HCV-CLD patients or healthy controls (Fig. 3c, d). Although the 8.9 k m/z peak was not identified as C3adesArg, it is possible that both the 8.1 and 8.9 k m/z peaks were specific tumor markers for HCC. Furthermore, we analyzed sera from 10 HCV-HCC patients who were diagnosed with HCC within 1 or 2 years and sera from five patients who had received curative treatments using RFA, PEIT, and TACE for HCC. The 8.1 k m/z C3a fragment in the HCV-HCC patients was significantly increased in the year of disease onset compared to the pre-onset year. After treatment, expression of the C3a fragment significantly decreased in all five of the patients who had measurable samples after treatment (Fig. 4a). In contrast, the 8.9 k m/z peak did not change regardless of the occurrence of HCC over time (Fig. 4b). Thus, the 8.1 k m/z C3a fragment appears to be the most discriminatory tumor marker for HCV-HCC.

Relationship between the C3a fragment and other tumor markers

AFP and DCP levels were measured in sera from 83 of 87 patients with HCV-associated liver disease. The recommended cutoff levels for these tumor markers, AFP and DCP, are 20 ng/ml and 40 mAU/ml, respectively. AFP-L3 in 26 patients with HCV-associated liver disease was also investigated among measurable samples in which AFP in a total 35 patients was higher than 20 ng/ml. The cutoff level of AFP-L3 was set at 10%. When samples from patients

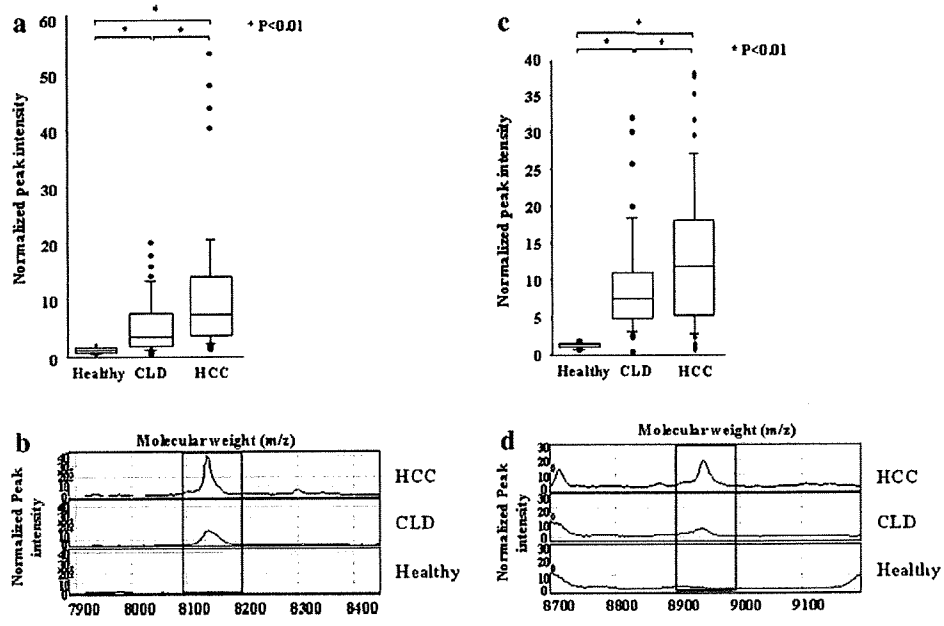

Fig. 3 **a** and **c** Comparisons of the expression profiles of the 8.1 and 8.9 k m/z peaks in HCV-HCC, HCV-CLD, and healthy sera. *Boxes* indicate the median ± 25th percentile. The *lower* and *upper bars* represent the 10th and 90th percentiles, respectively. **b** and **d** Representative spectra of the 8.1 and 8.9 k m/z peaks from patients in each group. The *horizontal axis* indicates the protein molecular weight, while the *vertical axis* designates the relative intensity

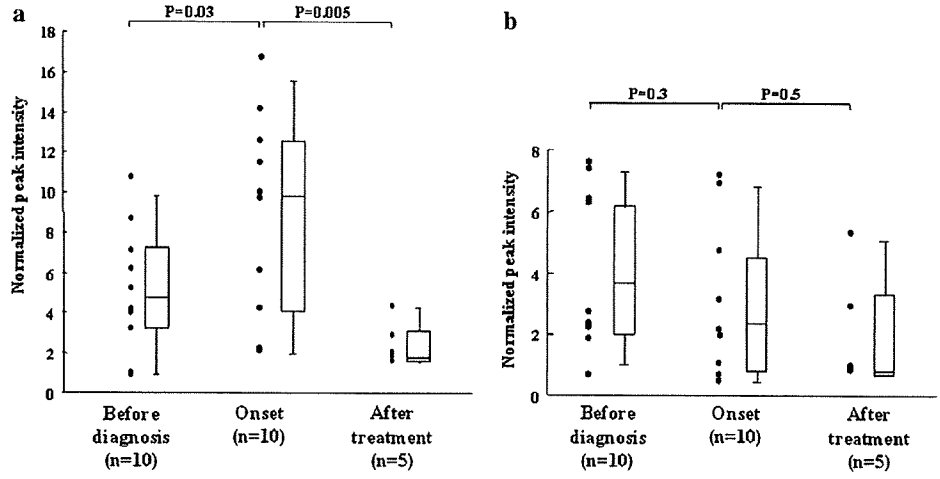

Fig. 4 Comparisons of the expression profiles of the 8.1 k m/z (**a**) and 8.9 k m/z (**b**) peaks in sera from HCV-HCC patients before diagnosis, during disease onset, and after treatment. The samples in the before diagnosis group included sera collected 1 or 2 years before the onset of HCC. *Boxes* indicate the median ± 25th percentile, the *lower bar* indicates the 10th percentile and the *upper bar* indicates the 90th percentile

Table 2 Diagnostic rates for hepatocellular carcinoma in the HCV infected patients

Markers	Sensitivity (%)	Specificity (%)	ROC AUC
AFP[a] (>20 ng/ml)	38 (17/45)	47 (18/38)	0.53
DCP[b] (>40 mAU/ml)	45 (20/44)	74 (29/39)	0.68
AFP-L3[c] (>10%)	58 (8/14)	50 (6/12)	0.58
C3a fragment (>3.5)	78 (37/45)	52 (22/42)	0.70
C3a fragment + AFP	91 (41/45)	26 (10/38)	0.72
C3a fragment + DCP	93 (41/44)	33 (13/39)	0.77
AFP + DCP	64 (28/44)	34 (12/35)	0.70
C3a fragment + AFP + DCP	98 (43/44)	20 (7/35)	0.80

[a] Alpha fetoprotein

[b] Des-γ-carboxy prothrombin

[c] Alpha fetoprotein, lectin lens culinaris agglutin-bound fraction

with HCV-HCC and HCV-CLD without HCC were compared, the sensitivity and specificity of AFP were 38 and 47%, whereas those of DCP were 45 and 74% and those of AFP-L3 were 58 and 50%, respectively. When the cutoff level for the relative intensity of the C3a fragment was set at 3.5, the sensitivity and specificity were 78 and 52%, respectively; the C3a fragment had the most sensitivity for the diagnosis of HCC. Furthermore, the ROC AUC of the C3a fragment, AFP, DCP, and AFP-L3 was 0.70, 0.53, 0.68, and 0.58, respectively (Table 2). There was no relationship between the C3a fragment and several other tumor and inflammation markers [AFP, DCP, AFP-L3, alanine aminotransferase (ALT), and high-sensitivity C-reactive protein (hs-CRP)], and each of these markers was independent of the diameter and number of tumors. The ROC AUC using AFP and DCP was highly similar to the ROC AUC with the C3a fragment alone. In addition, we investigated a combination assay that included the C3a fragment, AFP and DCP. This combination test, in which at least AFP, DCP, or the C3a fragment was positive, had a positive identification rate of 98%, although the specificity of this assay was too low at 20%. The ROC AUC of the combination test using AFP, DCP, and the C3a fragment was higher than those of any other markers. This result indicates that this combination assay using three markers is more useful than the combination assay using AFP ± DCP, which are measured worldwide to detect HCC (Table 2).

Profiling C3a expression in culture medium

C3a reacted with HCC cell lines, and the C3a peak in the culture medium was monitored by the ProteinChip system. The C3a fragment (approximately 8.1 k m/z) was not detected in the supernatants of HuH-7 and HepG2 cell cultures. However, the 8.9 k m/z peak was detected in the culture medium. This 8.9 k m/z peak was considered to be a stabilized form of C3a. This result indicated that the stabilized form of C3a (8.9 k m/z) was not undergoing proteasome-mediated degradation to yield the C3a fragment (8.1 k m/z) in these HCC cell lines.

Discussion

Because the HCC disease-associated mortality rate remains high, it is highly important to develop early diagnostic tools and treatments for HCC. Our study indicates that an 8.1 k m/z peak, which was identified as the C3a fragment by both peptide sequencing and an immunoassay, is up-regulated in the serum of HCC patients, 93% (42/45) of whom were TNM stage I or II. The C3a fragment in some HCC cases was also significantly higher in the year of HCC onset compared to the pre-onset year and decreased after curative treatment. Therefore, the C3a fragment appears to